arXiv:cond-mat/0609656v2 [cond-mat.stat-mech] 12 Feb 2007

# Spontaneous and induced dynamic fluctuations in glass-formers I: General results and dependence on ensemble and dynamics

L. Berthier,[1] G. Biroli,[2] J.-P. Bouchaud,[3,4] W. Kob,[1] K. Miyazaki,[5] and D. R. Reichman[5]

[1] *Laboratoire des Colloïdes, Verres et Nanomatériaux, UMR 5587, Université Montpellier II and CNRS, 34095 Montpellier, France*
[2] *Service de Physique Théorique Orme des Merisiers – CEA Saclay, 91191 Gif sur Yvette Cedex, France*
[3] *Service de Physique de l'État Condensé Orme des Merisiers – CEA Saclay, 91191 Gif sur Yvette Cedex, France*
[4] *Science & Finance, Capital Fund Management 6-8 Bd Haussmann, 75009 Paris, France*
[5] *Department of Chemistry, Columbia University, 3000 Broadway, New York, NY 10027, USA*

(Dated: February 6, 2008)

We study theoretically and numerically a family of multi-point dynamic susceptibilities that quantify the strength and characteristic lengthscales of dynamic heterogeneities in glass-forming materials. We use general theoretical arguments (fluctuation-dissipation relations and symmetries of relevant dynamical field theories) to relate the sensitivity of averaged two-time correlators to temperature and density to spontaneous fluctuations of the local dynamics. Our theoretical results are then compared to molecular dynamics simulations of the Newtonian, Brownian and Monte-Carlo dynamics of two representative glass-forming liquids, a fragile binary Lennard-Jones mixture and a model for the strong glass-former silica. We justify in detail the claim made in [Science, **310**, 1797 (2005)], that the temperature dependence of correlation functions allows one to extract useful information on dynamic lengthscales in glassy systems. We also discuss some subtle issues associated to the choice of microscopic dynamics and of statistical ensemble through conserved quantities, which are found to play an important role in determining dynamic correlations.

PACS numbers: 64.70.Pf, 05.20.Jj

## I. INTRODUCTION

Diverse materials, ranging from molten mixtures of metallic atoms, molecular and polymeric liquids, and colloidal suspensions may form glasses if sufficient undercooling or densification occurs [1, 2, 3]. A glass may be characterized mechanically as a solid, but microscopically lacks the long-range order of a crystal. Close to vitrification, the viscosity of glass-forming systems increases dramatically and sensitively as the thermodynamic control variables are changed. Furthermore, some degree of universality is observed in the thermal and temporal behavior of systems close to the glass transition, even though the material properties of such systems may be vastly different [1, 2]. Despite decades of intense theoretical and experimental work, the underlying causes of this interesting behavior are not well understood.

The observed quasi-universal behavior of glassy systems might be related to the existence of a growing lengthscale as the glass transition is approached. The search for such a correlation lengthscale has led to intense activity in recent years. Static structural indicators have repeatedly failed to show any evidence of collective behavior. Indeed, the static structure of a supercooled liquid hardly differs from that of the same liquid at relatively high temperatures. Clearly all simple structural correlations remain short-ranged as the glass transition is approached [4]. It has become manifest in the last decade that interesting behavior is revealed by spatially correlated *dynamics*. As a whole, such effects are referred to as 'dynamical heterogeneity' [5, 6, 7, 8, 9].

The investigation, via theory [10, 11, 12, 13, 14, 15, 16, 17], simulation [18, 19, 20, 21], and experiment [22, 23, 24, 25, 26, 27], of various aspects of dynamic heterogeneity has greatly advanced our understanding of the behavior of systems close to the glass transition. In particular, multi-point susceptibilities have been devised to quantify the behavior and magnitude of the putative growing dynamical lengthscale [8, 15, 16, 18, 20, 28, 29, 30, 31, 32, 33, 34], and experimental studies have, for several materials, directly determined the number of molecular units that move cooperatively near the glass transition [22, 23, 25, 26, 35, 36, 37]. Despite recent breakthroughs, much more work needs to be done to fully characterize such a behavior both experimentally and theoretically.

In the present work, contained here and in a companion paper [38], we make a step towards this goal by investigating in detail different susceptibilities that may be categorized according to the induced or spontaneous nature of the measured fluctuations [37]. Spontaneous dynamic fluctuations can be characterized by four-point functions, as proposed and studied earlier [8, 15, 16, 18, 20, 28, 29, 30, 31, 32, 33, 34], or three-point functions, as in [37, 39]. Instead, fluctuations can be *induced* by monitoring the change of dynamical correlators that follows a change of an external control parameter, e.g. temperature [37, 39]. As we shall show, it is possible to relate induced and spontaneous dynamical fluctuations via fluctuation-dissipation relations as proposed in [37]. This provides a very valuable experimental tool to measure dynamic fluctuations since, as usual, induced fluctuations are much easier to measure than spontaneous ones.

Using molecular dynamics simulations of different

archetypal glass-forming liquids (e.g. "strong" materials that exhibit an Arrhenius temperature dependence of the viscosity, and "fragile" ones, whose viscosity displays a super-Arrhenius temperature dependence) we shall show that in the slow dynamical regime a considerable fraction of spontaneous fluctuations can be attributed to energy fluctuations: since the dynamics is spatially correlated a local energy fluctuations induces a change in the dynamics over a much larger range.

Our analysis will however reveal that *global* four-point correlations describing the fluctuations of intensive dynamical correlators may depend both on the statistical ensemble and on the underlying microscopic dynamics. *Local* four-point correlations measuring the correlation between the relaxation dynamics at a finite distance apart of course do not depend on the statistical ensemble but they do depend on the underlying microscopic dynamics. This is striking because it is known that correlators measuring the average dynamics do not depend in the relevant glassy regime on the microscopic dynamics (Newtonian or stochastic [40, 41]). We address this problem both theoretically and numerically, and conclude that, although the underlying physical mechanisms are the same, dynamical correlations depend quantitatively on the conserved physical quantities (and global four-point correlations even on the statistical ensemble). For example, the absolute magnitude of global spontaneous dynamical fluctuations in a Lennard-Jones system in the $NVT$ ensemble obtained from Brownian dynamics (BD) or Monte-Carlo dynamics (MC) are very similar, but are considerably smaller than that obtained with Newtonian dynamics (ND) in the same $NVT$ ensemble, whereas ND simulations performed in the $NVE$ ensemble yield results that are close to the BD and MC results in the $NVT$ ensemble. However, we stress that all our results point toward the conclusion that the behaviour of all these quantities as the glass transition is approached is governed by the growth of a *unique* dynamic correlation length, at least in the numerically accessible regime.

The aim of the present paper is to provide the reader with the physical picture underlying the dynamical susceptibilities introduced in [37], along with more technical elements based on general field-theoretical considerations and detailed numerical investigations of different realistic glass-forming liquids. In a companion paper [38], we present some quantitative predictions for these susceptibilities, obtained within different theoretical models: mean-field spin glass models [42], mode-coupling theory [43], and kinetically constrained models [44] which we again confront with the results from molecular dynamics simulations. The present paper is arranged in four sections. In Section II we present the physical motivations, definitions and physical content of several multi-point dynamic susceptibilities. We derive in particular general results for the ensemble dependence of dynamic fluctuations, fluctuation-dissipation relations, and bounds between induced and spontaneous dynamic fluctuations. In Section III we present a field-theoretic derivation of the behavior of dynamic fluctuations for various types of microscopic dynamics. This is particularly useful in identifying the precise physical mechanism leading to a growth of dynamic correlations, and the dependence of multipoint susceptibilities on the microscopic dynamics. In Section IV we summarize our various theoretical predictions and extract some important consequences, relevant to experiments, that need to be tested numerically. In Section V we present the results of detailed molecular dynamics simulations of two model glass-forming liquids, a fragile binary Lennard-Jones mixture and the strong BKS model for silica. We compare spontaneous and induced fluctuations and show that, as predicted theoretically, dynamic correlations strongly depend on the choice of microscopic dynamics and statistical ensemble. Our results suggest, however, that a unique dynamical lengthscale governs the growth of dynamical susceptibilities in all cases. In Section VI we give the conclusions of our study. Although very natural in spin-systems, four-point correlators in liquids mix dynamical heterogeneities with different physical effects (in particular, energy and density conservation) and might therefore not be the most effective object to work with. On the other hand, we fully confirm the claim made in [37], that the temperature dependence of correlation functions allows one to extract rich and useful information on dynamic lengthscales in glassy systems [45].

## II. MULTI-POINT DYNAMIC CORRELATORS AND NEW LINEAR SUSCEPTIBILITIES

### A. Why four-point correlators? The spin glass case

No static correlation has yet been found to reveal any notable feature upon approaching the glass transition [4, 46]. Any lengthscale associated with the slowing down of the system must therefore be hidden in some dynamic correlation function. This issue is in fact deeply related to one of the most important question pertaining to the physics of disordered systems – how can one define *long-range amorphous order* in such systems?

We know from the theory of spin glasses that the above oxymoron has in fact a precise answer: some hidden long-range order indeed develops at the spin glass transition [47]. In order to reveal this long-range order, conventional two-point functions are useless. Even if spins $s_{\mathbf{x}}$ and $s_{\mathbf{x+y}}$ have non-zero static correlations $\langle s_{\mathbf{x}} s_{\mathbf{x+y}} \rangle$ in the spin glass phase, the average over space for a given distance $y$ vanishes because the pairwise correlations randomly change sign whenever $\mathbf{x}$ changes. The insight of Edwards and Anderson is that one should first square $\langle s_{\mathbf{x}} s_{\mathbf{x+y}} \rangle$ before averaging over space [48]. In this case, the resulting (four-spin) correlation function indeed develops long-range tails in the spin glass phase. This correlation in fact decays so slowly that its volume integral, related to the non-linear magnetic susceptibility of the material, diverges in the whole spin glass phase [49].

The Edwards-Anderson idea can in fact be understood from a dynamical point of view, which is important for understanding both the physics of the spin glass just above the transition, and its generalization to structural glasses. Consider, in the language of spins, the following four-point correlation function:

$$S_4(\mathbf{y},t) = [\langle s_{\mathbf{x}}(t=0)s_{\mathbf{x}+\mathbf{y}}(t=0)s_{\mathbf{x}}(t)s_{\mathbf{x}+\mathbf{y}}(t)\rangle]_x, \quad (1)$$

where the brackets $[...]_x$ indicate a spatial average. Suppose that spins $s_{\mathbf{x}}$ and $s_{\mathbf{x}+\mathbf{y}}$ develop static correlations $\langle s_{\mathbf{x}}s_{\mathbf{x}+\mathbf{y}}\rangle$ within the glass phase. In this case, $S_4(\mathbf{y}, t \to \infty)$ will clearly converge to the spin glass correlation $[\langle s_{\mathbf{x}}s_{\mathbf{x}+\mathbf{y}}\rangle^2]_x$. More generally, $S_4(\mathbf{y},t)$ for finite $t$ is able to detect *transient* tendencies to spin glass order, for example slightly above the spin glass transition temperature $T_c$. Close to the spin glass transition, both the persistence time and the dynamic length diverge in a critical way:

$$S_4(\mathbf{y},t) \approx y^{2-d-\eta}\hat{S}\left(\frac{y}{\xi},\frac{t}{\tau}\right), \quad (2)$$

where $\xi \sim (T-T_c)^{-\nu}$ and $\tau \sim (T-T_c)^{-z\nu}$. As mentioned above, the static non-linear susceptibility diverges as $\int d\mathbf{y} S_4(\mathbf{y}, t \to \infty) \sim \xi^{2-\eta}$. More generally, one can define a time-dependent dynamic susceptibility as:

$$\chi_4(t) \equiv \int d\mathbf{y}\ S_4(\mathbf{y},t), \quad (3)$$

which defines, provided $S_4(\mathbf{0},t) \sim 1$, a correlation volume, i.e. the typical number of spins correlated in dynamic events taking place over the time scale $t$. As we shall discuss below, $\chi_4(t)$ can also be interpreted as a quantitative measure of the dynamic fluctuations. Note however that the precise relation between $\chi_4$ and $\xi$ depends on the value of the exponent $\eta$, which is physically controlled by the detailed spatial structure of $S_4$:

$$\chi_4(t=\tau) \propto \xi^{2-\eta}. \quad (4)$$

Therefore, spin glasses offer a precise example of a system which gets slower and slower upon approaching $T_c$ but without any detectable long-range order appearing in two-point correlation functions. Only more complicated four-point functions are sensitive to the genuine amorphous long-range order that sets in at $T_c$ and give non-trivial information even above $T_c$. In the case of spin glasses it is well established that the transition is related to the emergence of a low temperature spin glass phase. In the case of the glass transition of viscous liquids the situation is much less clear. There might be no true phase transition toward a low temperature amorphous phase. It is still reasonable to expect that the dramatic increase of the relaxation time is due to a transient amorphous order that sets in and whose range grows approaching the glass transition. Growing timescales should be somehow related to growing lengthscales [50]. A good candidate to unveil the existence of this phenomenon is the function $S_4(\mathbf{y},t)$ introduced previously, since nothing in the above arguments was specific to systems with quenched disorder. The only difference is that although transient order is detected in $S_4(\mathbf{y},t)$ or its volume integral $\chi_4(t)$ for times of the order of the relaxation time, in the long time limit these two functions may not, and indeed do not in the case of supercooled liquids, show long-range amorphous order. This roots back to the different nature of the glass and spin glass transitions (see the discussion in [49]).

### B. Supercooled liquids and more multi-point correlations

In the case of liquids, we may consider a certain space dependent observable $o(\mathbf{x},t)$, such as, for example, the local excess density $\delta\rho(\mathbf{x},t) = \rho(\mathbf{x},t) - \rho_0$, where $\rho_0$ is the average density of the liquid, or the local dipole moment, the excess energy, etc. We will assume in the following that the average of $o(\mathbf{x},t)$ is equal to zero, and the variance of $o(\mathbf{x},t)$ normalized to unity. The dynamic two-point correlation is defined as:

$$C_o(\mathbf{r},t) = [o(\mathbf{x},t=0)o(\mathbf{x}+\mathbf{r},t)]_x, \quad (5)$$

where the normalization ensures that $C_o(\mathbf{r}=\mathbf{0},t=0) = 1$. The Fourier transform of $C_o(\mathbf{r},t)$ defines a generalized dynamic structure factor $S_o(\mathbf{k},t)$ [51]. All experimental and numerical results known to date suggest that as the glass transition is approached, no spatial anomaly of any kind appears in $C_o(\mathbf{r},t)$ (or in $S_o(\mathbf{k},t)$) although of course there could still be some signal which is perhaps too small to be measurable. The only remarkable feature is that the slowing down of the two-point correlation functions often obeys, to a good approximation, "time-temperature superposition" in the $\alpha$-relaxation regime $t \sim \tau_\alpha$, i.e.:

$$C_o(\mathbf{r},t) \approx q_o(\mathbf{r}) f\left(\frac{t}{\tau_\alpha(T)}\right), \quad (6)$$

where $q_o$ is often called the non-ergodicity (or Edwards-Anderson) parameter, and the scaling function $f(x)$ depends only weakly on temperature. This property will be used to simplify the following discussions, but it is not a crucial ingredient.

Whereas $C_o(\mathbf{r},t)$ measures how, on average, the dynamics decorrelates the observable $o(\mathbf{x},t)$, it is natural to ask whether this decorrelation process is homogeneous is space and in time. Can the correlation last much longer than average? In other words, what is the distribution (over possible dynamical histories) of the correlation $C_o(\mathbf{r},t)$? Clearly, since $C_o(\mathbf{r},t)$ is defined as an average over some large volume $V$, the variance $\Sigma_C^2$ of $C_o(\mathbf{r},t)$ is expected to be of order $\xi^{2-\eta}/V$, where $\xi$ is the lengthscale over which $C_o(\mathbf{r},t)$ is significantly correlated.

More precisely we define:

$$\Sigma_C^2 = \int \frac{d\mathbf{x}}{V}\frac{d\mathbf{x}'}{V} o(\mathbf{x},0)o(\mathbf{x}+\mathbf{r},t)o(\mathbf{x}',0)o(\mathbf{x}'+\mathbf{r},t) - C_o(\mathbf{r},t)^2, \quad (7)$$

which, using translational invariance, can be transformed into the space integral of a four-point correlation:

$$\Sigma_C^2 = \int \frac{d\mathbf{y}}{V} S_4(\mathbf{y},t), \quad (8)$$

where

$$S_4(\mathbf{y},t) = \Big\{ [o(\mathbf{x},0)o(\mathbf{x}+\mathbf{r},t)o(\mathbf{x}+\mathbf{y},0)o(\mathbf{x}+\mathbf{y}+\mathbf{r},t)]_x - [o(\mathbf{x},t=0)o(\mathbf{x}+\mathbf{r},t)]_x^2 \Big\}. \quad (9)$$

The variance of $C_o(\mathbf{r},t)$ can thus be expressed as an integral over space of a four-point correlation function, which measures the spatial correlation of the temporal correlation. This integral over space is also the Fourier transform of $S_4(\mathbf{y},t)$ with respect to $\mathbf{y}$ at the wavevector $\mathbf{q}$ equal to zero. We want to insist at this stage that $\mathbf{r}$ and $\mathbf{y}$ in the above equations play very different roles: the former enters the very definition of the correlator we are interested in Eq. (5), whereas the latter is associated with the scale over which the dynamics is potentially correlated. Correspondingly, great care will be devoted in the following to distinguish the wavevector $\mathbf{k}$, conjugate to $\mathbf{r}$, and $\mathbf{q}$ conjugate to $\mathbf{y}$.

Specializing to the case $\mathbf{r} = 0$ (local dynamics), one finally obtains [87]:

$$\Sigma_C^2 \equiv \frac{\chi_4(t)}{N}. \quad (10)$$

The analogy with spin glasses developed above suggests that this quantity reveals the emergence of amorphous long-range order; it is in fact the natural diverging susceptibility in the context of $p$-spin descriptions of supercooled liquids, where a true dynamical phase transition occurs at a certain critical temperature [17, 28, 38, 39, 52]. Since in real systems no true phase transition is observed, one expects $\chi_4(t)$ to grow until $t \approx \tau_\alpha$ and decay back to zero thereafter. Until $\tau_\alpha$, there cannot be strong differences between a system with quenched disorder and a system where disorder is dynamically self-induced.

However, contrary to spin glasses, for which an underlying lattice structure exists, viscous liquids consist of molecules or atoms having continuum positions. As a consequence, one has to coarse-grain space in order to measure the fluctuations of the local relaxation dynamics. Local now means on a region of the order of the interparticle distance. Therefore, generically, $\chi_4(t) = V\Sigma_C^2$ correspond either to the fluctuations of the Fourier transform of $C_o(\mathbf{r},t)$ evaluated at a wave-vector, $k_0$, of the order of the first peak in the structure factor [33], or to a spatial average $\int d\mathbf{r} C_o(\mathbf{r},t)w(\mathbf{r})$ where $w(\mathbf{r})$ is an overlap function equal to one for lengths of the order of $2\pi/k_0$ and zero otherwise [8]. The dependence of dynamical correlations on the coarse-graining length has been recently studied in [53] and is also discussed in the companion paper [38].

Although readily accessible in numerical simulations, $\Sigma_C^2$ is in general very small and impossible to measure directly in experiments, except when the range of the dynamic correlation is macroscopic, as in granular materials [36] or in soft glassy materials where it can reach the micrometer and even millimeter range [35, 54]. The central idea of this work is that induced dynamic fluctuations are more easily accessible than spontaneous ones, and can be related to one another by fluctuation-dissipation theorems. The physical motivation is that while four-point correlations offer a direct probe of the dynamic heterogeneities, other multi-point correlation functions give very useful information about the microscopic mechanisms leading to these heterogeneities. For example, one expects that the slow part of a local enthalpy (or energy, density) fluctuation per unit volume $\delta h$ at $\mathbf{x}$ and time $t = 0$ triggers or eases the dynamics in its surroundings, leading to a systematic correlation between $\delta h(\mathbf{x}, t = 0)$ and $o(\mathbf{x}', t = 0)o(\mathbf{x}' + \mathbf{r}, \tau_\alpha)$. This defines a family of three-point correlation functions that relate thermodynamic or structural fluctuations to dynamics. Interestingly, some of these three-point correlations are both experimentally accessible and give bounds or approximations to the four-point dynamic correlations. The reason is as follows. In the same way that the space integral of the four-point correlation function is the variance of the two-point correlation, the space integral of the above three-point correlation is the covariance of the dynamic correlation with the energy fluctuations [88]:

$$\Sigma_{CH} = \frac{1}{VN}\int d\mathbf{x}\, d\mathbf{x}' o(\mathbf{x}'+\mathbf{r},t)o(\mathbf{x}',0)\delta h(\mathbf{x},0) \equiv \frac{1}{N}\int d\mathbf{y}\, [o(\mathbf{x}+\mathbf{y}+\mathbf{r},t)o(\mathbf{x}+\mathbf{y},0)\delta h(\mathbf{x},0)]_x. \quad (11)$$

Hence, using the fact that the enthalpy fluctuations per particle are of order $\sqrt{c_P}k_BT$ (where $c_P$ is the specific heat in $k_B$ units), the quantity $N\Sigma_{CH}/\sqrt{c_P}k_BT$ defines the *number of particles* over which enthalpy and dynamics are correlated. Of course, analogous identities can be derived for the covariance with density (and energy) fluctuations.

Now, on very general grounds, the covariance obeys the Cauchy-Schwarz bound: $\Sigma_{CH}^2 \leq \Sigma_C^2\Sigma_H^2$, where $\Sigma_H^2$ is the variance of the enthalpy fluctuations, equal to $c_P(k_BT)^2/N$ in the $NPT$ ensemble, $N = \rho_0 V$ being the total number of particles. Therefore, the dynamic susceptibility $\chi_4(t)$ is bounded from below by:

$$\chi_4(t) \equiv N\Sigma_C^2 \geq \frac{N^2\Sigma_{CH}^2}{N\Sigma_H^2} = \left(\frac{N\Sigma_{CH}}{\sqrt{c_P}(k_BT)}\right)^2, \quad (12)$$

where, as we show below, the right hand side can be accessed experimentally. We then discuss in Sec. II E how the above bound can be interpreted as an approximation, with corrections that can be physically estimated. Note that we chose here $\chi_4(t)$ to define a number of particles; one can of course convert it into a volume by multiplying $\chi_4$ by $v_0 = 1/\rho_0$, the average volume per particle. Note also that here and in the following we will work in the $NPT$ ensemble which is the relevant ensemble for experiments on molecular liquids. We will discuss later the generalization to different ensembles.

### C. A dynamic fluctuation-dissipation theorem and growing lengthscales

Consider a system in the grand-canonical $NPT$ ensemble. The probability of a given configuration $\mathcal{C}$ is given by the Boltzmann weight $\exp(-\beta H[\mathcal{C}])/Z$, where $\beta = 1/k_B T$ and $Z$ is the grand-partition function. Suppose one studies an observable $O$ with the following properties: (i) $O$ only depends on the current microscopic configuration $\mathcal{C}$ of the system and (ii) $O$ can be written as a sum of local contributions:

$$O = \frac{1}{V}\int d\mathbf{x}\; o(\mathbf{x}). \tag{13}$$

In this case, a well-known static fluctuation-dissipation theorem holds [51]:

$$\frac{\partial \langle O\rangle}{\partial \beta} = -\int d\mathbf{x}\, \langle o(\mathbf{x})\delta h(\mathbf{0})\rangle \equiv -N\Sigma_{OH}, \tag{14}$$

where we decomposed the enthalpy in a sum of local contributions as well [51].

Interestingly, in the case of *deterministic* Hamiltonian dynamics, the value of any local observable $o(\mathbf{x},t)$ is in fact a highly complicated function of the initial configuration at time $t = 0$. Therefore, the correlation function, now averaged over both space and initial conditions can be written as a thermodynamical average:

$$C_o(\mathbf{r},t;T) = \frac{1}{Z(\beta)V}\int d\mathbf{x}\; o(\mathbf{x}+\mathbf{r},t)o(\mathbf{x},t=0) \times \exp\left[-\beta\int d\mathbf{x}'\; h(\mathbf{x}',t=0)\right]. \tag{15}$$

Hence, the derivative of the correlation with respect to temperature (at fixed volume) directly leads, in the case of purely conservative Hamiltonian dynamics, to the covariance between initial energy fluctuations and the dynamical correlation. Defining $S_T(\mathbf{x},t) = \langle o(\mathbf{x}+\mathbf{r},t)o(\mathbf{x},0)\delta h(\mathbf{0},0)\rangle$, one finds:

$$\frac{\partial C_o(\mathbf{r},t;T)}{\partial T} = \frac{1}{k_B T^2}\int d\mathbf{x}\; S_T(\mathbf{x},t) \equiv \chi_T(\mathbf{r},t). \tag{16}$$

Hence, the sensitivity of the dynamics to temperature $\chi_T$ is directly related to a dynamic correlation. This last equality, although in a sense trivial, is one of the central result of this work. It has an immediate deep physical consequence, which is the *growth of a dynamical length upon cooling in glassy systems*, as we show now.

Define $\tau_\alpha(T)$ such that $C_o(\mathbf{0}, t=\tau_\alpha; T) = e^{-1}$ (say). Differentiating this definition with respect to $T$ gives

$$0 = \frac{d\tau_\alpha}{dT}\frac{\partial C_o(\mathbf{0},t=\tau_\alpha;T)}{\partial t} + \frac{\partial C_o(\mathbf{0},t=\tau_\alpha;T)}{\partial T}. \tag{17}$$

Since $C_o(\mathbf{0},t;T)$ decays from 1 to zero over a time scale $\tau_\alpha$, one finds that generically, using Eq. (16):

$$\int d\mathbf{x}\; \frac{\langle o(\mathbf{x},t=\tau_\alpha)o(\mathbf{x},0)\delta h(\mathbf{0},0)\rangle}{\rho_0\sqrt{c_P}k_B T} \sim \frac{1}{\rho_0\sqrt{c_P}}\frac{d\ln\tau_\alpha}{d\ln T}. \tag{18}$$

Now, $\delta h$ is of order $\rho_0\sqrt{c_P}k_B T$ and $\langle o^2\rangle$ is normalized to unity, and the quantity $\chi_0 \equiv S_T(\mathbf{0},\tau_\alpha)/\rho_0\sqrt{c_P}k_B T$ cannot appreciably exceed unity. The above integral can be written as $\chi_0 v_T$, which defines a volume $v_T$ over which enthalpy fluctuations and dynamics are appreciably correlated. Note that the interpretation of $v_T$ as a true correlation volume requires that $\chi_0$ be of order one, and its increase is only significant if $\chi_0$ is essentially temperature independent. If this is not the case, then the integral defined in (18) could grow due to a growing $\chi_0$ and not a growing length, which would obviate the notion that $v_T$ is a correlation volume. For now we will assume these properties hold, and return to this crucial point theoretically in more detail in Sec.IV and with direct numerical evidence in Sec.V.

Assuming $\chi_0 \leq 1$, a divergence of the right hand side of the equality (16) necessarily requires the growth of $v_T$. More precisely, as soon as $\tau_\alpha$ increases faster than any inverse power of temperature, the slowing down of a Hamiltonian system is necessarily accompanied by the growth of a dynamic correlation length. However, as already mentioned above, the precise relation between $\partial C/\partial \ln T$ and an actual *lengthscale*, $\xi$, depends on the value and structure of the spatial correlation function (for example the value of $\chi_0$ and the exponent $\eta$). In the simplest case of an exponentially decaying $S_T(\mathbf{x},t)$, one finds:

$$T\frac{\partial C_o(\mathbf{r},t;T)}{\partial T} = 8\pi\sqrt{c_V}\chi_0\rho_0\xi^3 \tag{19}$$

It is instructive to study the case of a strong glass-former, for which the slowing down is purely Arrhenius, i.e $\tau_\alpha = \tau_0\exp[\Delta/(k_B T)]$, where $\Delta$ is some activation barrier. The volume $v_T$ is then given by:

$$v_T \sim \left|\frac{d\ln\tau_\alpha}{d\ln T}\right| = \frac{\Delta}{k_B T}, \tag{20}$$

which increases as the temperature is decreased, and diverges as $T \to 0$. This is at first sight contrary to intuition since simple barrier activation seems to be a purely local process. However, one should remember that the dynamics strictly conserves energy, so that the energy used to cross a barrier must be released from other parts

of the system. This release necessarily induces dynamic correlations between the Arrheniusly relaxing objects. We conclude that even in a strong glass the Arrhenius slowing down is necessarily accompanied by the growth of a dynamic lengthscale. Note again that this conclusion relies on subsidiary conditions that must be met. Indeed, it is not difficult to find examples of model Newtonian systems for which $|d\ln\tau_\alpha/d\ln T|$ grows substantially even though the physics is entirely local. In such cases, however, it is expected that the spatial structure of $S_T(\mathbf{x},t)$ will be trivial, and the condition $\chi_0 \leq 1$ (independent of temperature) will be violated. In computer simulations, these conditions may be checked, as we do in Sec.V.

When the relaxation time diverges in a Vogel-Fulcher manner, i.e. $\tau_\alpha = \tau_0 \exp[DT_0/(T-T_0)]$, one finds that the corresponding dynamic correlation volume also diverges at $T_0$, as:

$$v_T(\tau_\alpha) \sim \frac{DTT_0}{(T-T_0)^2} \propto (\ln\tau_\alpha)^2, \qquad (21)$$

where the last estimate holds sufficiently close to $T_0$.

More generally, one can study the behavior of $\chi_T(\mathbf{0},t) \sim \partial C_o(\mathbf{0},t;T)/\partial T$ as a function of time. Since at all temperature $C_o(\mathbf{0},t=0;T)=1$ and $C_o(\mathbf{0},\infty;T)=0$, it is clear that $\chi_T(\mathbf{0},t)$ is zero at short and long times. We illustrate in Fig. 1 the shape of $\chi_T(\mathbf{0},t)$ for two glass-formers studied by molecular dynamics simulations described in Sec. V. It has a peak for $t \approx \tau_\alpha$. It is a useful exercise to study the example where the correlation function is a stretched exponential with exponent $\beta$ [not to be confused with $1/k_BT$], in which case:

$$\frac{\partial C_o(\mathbf{0},t;T)}{\partial \ln T} = \frac{d\ln\tau_\alpha}{d\ln T}\ \beta\left(\frac{t}{\tau_\alpha}\right)^\beta \exp\left[-\left(\frac{t}{\tau_\alpha}\right)^\beta\right]. \qquad (22)$$

This function behaves as a power-law, $t^\beta$, at small times and reaches a maximum for $t=\tau_\alpha$, before decaying to zero. The power-law at small times appears in the context of many different models, as discussed for the time behavior of $\chi_4(t)$ [34]. Note also that for $t=\tau_\alpha$ and $T=T_g$, one has:

$$\left.\frac{\partial C_o(\mathbf{0},\tau_\alpha;T)}{\partial \ln T}\right|_{T_g} = \beta\, m\, \ln 10, \qquad (23)$$

where $m = Td\log_{10}\tau_\alpha/dT|_{T_g}$ is the steepness index, which characterizes the fragility of the glass. Note that in many cases, the resulting numerical value of $v_T \propto \chi_T$ turns out to be already large in the late $\beta$-regime, meaning that the concept of a cage is misleading because caging if fact involves the correlated motion of many particles [36, 39].

Using the inequality in Eq. (12) with the results of the present section, we finally obtain a lower bound on the dynamical susceptibility $\chi_4(t)$ for Newtonian systems in the $NPT$ ensemble, which is experimentally accessible:

$$\chi_4(\mathbf{r},t) \geq \frac{T^2\chi_T^2(\mathbf{r},t)}{c_P} = \frac{1}{c_P}\left(\frac{\partial C_o(\mathbf{r},t;T)}{\partial \ln T}\right)_P^2. \qquad (24)$$

This bound implies that as soon as $\chi_T$ increases faster than $T^{-1}$ at low temperatures, $\chi_4$ will eventually exceed unity; since $\chi_4$ is the space integral of a quantity bounded from above, this again means that the lengthscale over which the four-point correlation $S_4(y,\tau_\alpha)$ extends *has to grow* as the system gets slower and slower. More quantitative statements require information on the amplitude and shape of $S_4(y,\tau_\alpha)$ which general field-theoretical and numerical results provide.

The above result in Eq. (24) is extremely general and applies to different situations discussed in the next section. It however does *not* apply when the dynamics is not Newtonian, as for instance for Brownian particles or in Monte-Carlo numerical simulations [41, 55, 56]. The reason is that in these cases, not only the initial probability but also the transition probability from the initial to the final configuration itself explicitly depends on temperature. In Brownian dynamics, for example, the noise in the Langevin equation depends on temperature [55]. Hence, $\partial C_o(\mathbf{r},t;T)/\partial T$ receives extra contributions from the whole trajectory, that depend on the explicit choice of dynamics. We will argue below that when a dynamical critical point exists or is narrowly avoided, a system with Brownian dynamics should display dynamical correlations of the form $\chi_4 \sim \chi_T$ rather than the scaling $\chi_4 \sim \chi_T^2$ suggested by the above bound, Eq. (24).

### D. Several generalizations

#### 1. Density rather than temperature

In the above section, we have shown that the response of the correlator to a change of temperature is related to dynamic correlations. Other perturbing fields may also be relevant, such as density, pressure, concentration of species in the case of mixtures, etc. For example, for hard-sphere colloids, temperature plays very little role whereas small changes of density can lead to enormous changes in relaxation times [57]. Using the expression for the probability of initial configurations in the $NPT$ ensemble, and the fact that the dynamics only depends on the initial condition, one now derives the following equality:

$$\left.\frac{\partial C_o(\mathbf{r},t;P)}{\partial P}\right|_T = -\frac{\rho_0}{k_BT}\int d\mathbf{x}\ \langle o(\mathbf{x}+\mathbf{r},t)o(\mathbf{x},0)\delta v(\mathbf{0},0)\rangle, \qquad (25)$$

which can again be used to define a dynamic correlation volume $\chi_\rho$. Introducing the isothermal compressibility $\kappa_T = (\partial\rho/\partial P)|_T/\rho_0$ and noting that the total variance of volume fluctuations per particle is given by $k_BT\kappa_T/\rho_0$, we find:

$$\begin{aligned} N\Sigma_{CV} &= \rho_0 \int d\mathbf{x}\ \langle o(\mathbf{x}+\mathbf{r},t)o(\mathbf{x},t=0)\delta v(\mathbf{0},t=0)\rangle \\ &= -k_BT\kappa_T \left.\frac{\partial C_o(\mathbf{r},t;\rho)}{\partial\ln\rho}\right|_T, \end{aligned} \qquad (26)$$

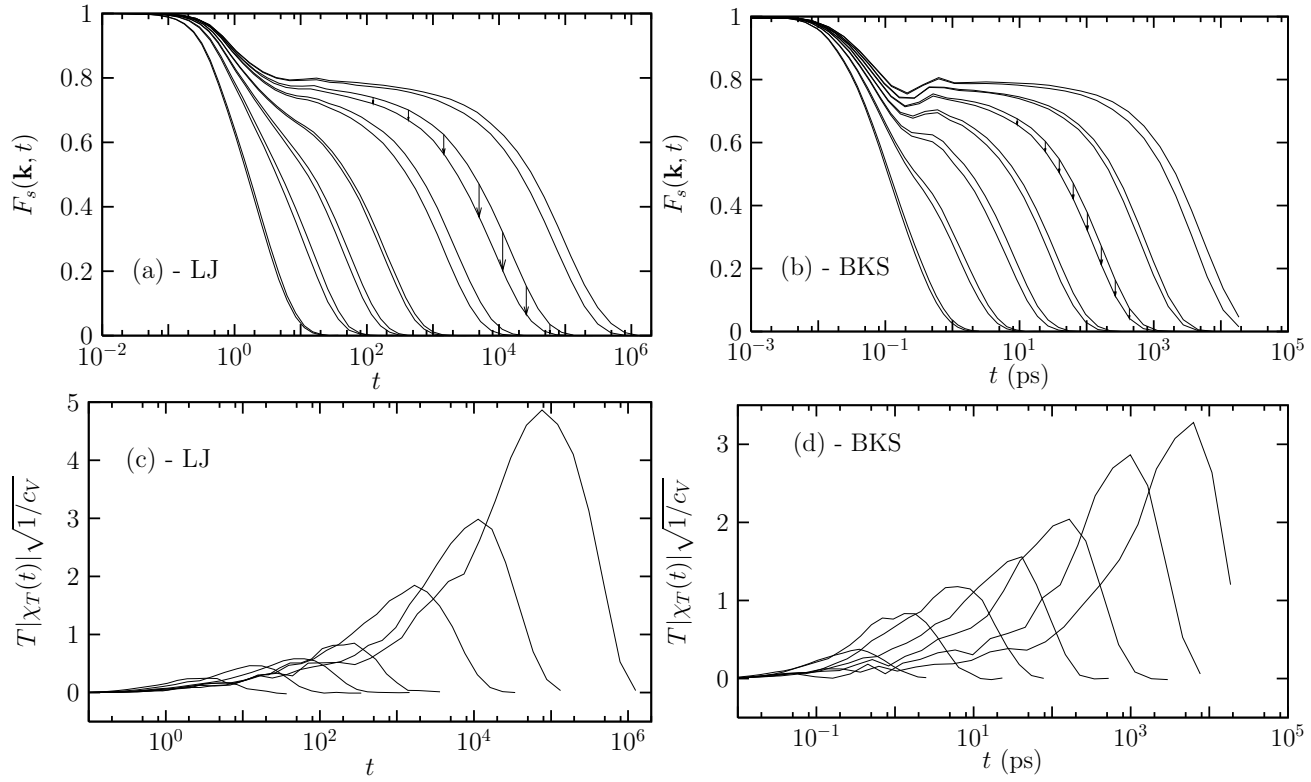


FIG. 1: (a) and (b) respectively show the self-intermediate scattering functions $F_s(\mathbf{k},t)$ as a function of time for various temperatures in a binary Lennard-Jones mixture and the BKS model for silica, obtained from the molecular dynamics numerical simulations discussed in Sec. V. (a) $T = 2.1$, 2.0, 1.05, 1.0, 0.75, 0.72, 0.61, 0.6, 0.51, 0.5, 0.47, 0.46, 0.435 and 0.43 from left to right. (b) $T = 6100$, 5900, 4700, 4600, 4000, 3920, 3580, 3520, 3250, 3200, 3000, 2960, 2750, and 2715 K from left to right. The arrows illustrate how $\chi_T = \partial F_s/\partial T$ is obtained by finite difference for each pair of temperatures. (c) and (d) show the resulting $\chi_T(t)$ for both models, normalized by the strength of energy fluctuations. We show the absolute value since $\chi_T$ is a negative quantity. In both liquids the dynamic susceptibility presents a peak for $t \approx \tau_\alpha$ whose height increases as temperature decreases, revealing increasingly heterogeneous and spatially correlated dynamics.

from which we deduce a second bound on the dynamic correlation volume $\chi_4(t)$:

$$\chi_4(\mathbf{r},t) \geq \rho_0 k_B T \kappa_T \left( \frac{\partial C_o(\mathbf{r},t;\rho)}{\partial \ln \rho} \right)_T^2 . \qquad (27)$$

Again, the right hand side of this expression is accessible to experiments [37]. Very importantly, and contrarily to the case of temperature, this inequality holds even for Brownian dynamics since the statistics of trajectories have no explicit dependence on pressure or density. Finally, a similar inequality holds for binary mixtures, relating $\chi_4(t)$ to the dependence of the correlation function on the mixture composition.

### 2. *Correlation and response in frequency space*

We have considered up to now the variance of the correlation function for a given time $t$, related to the four-point susceptibility $\chi_4(t)$, but this can be generalized to the covariance of the correlation in frequency space.

Defining $\hat{C}_o(\mathbf{r},\omega) = \int_0^\infty dt \cos(\omega t) C_o(\mathbf{r},t)$, the fluctuations of $\hat{C}_o(\mathbf{r},\omega)$ define a four-point susceptibility in Fourier space $\chi_4(\mathbf{r},\omega)$ given by:

$$\chi_4(\mathbf{r},\omega) = N \Sigma_{\hat{C}\hat{C}} \qquad (28)$$

Repeating the same argument developed for correlations in time space, one finds:

$$\chi_4(\mathbf{r},\omega) = \frac{1}{c_P} \left( \frac{\partial C_o(\mathbf{r},\omega;T)}{\partial \ln T} \right)^2 . \qquad (29)$$

We have up to now considered correlation functions, but the very same string of arguments also applies to linear response functions, which can, in the context of Newtonian dynamics, be written solely as functions of the initial condition. For example, the susceptibility of the observable $o$ to an external field $X$ is:

$$\chi_o(\mathbf{r},t) = \frac{1}{Z(\beta)V} \int d\mathbf{x} \, \frac{\delta o(\mathbf{x}+\mathbf{r},t)}{\delta X(\mathbf{x},t=0)} \times \exp\left[ -\beta \int d\mathbf{x}' \, h(\mathbf{x}',t=0) \right], \qquad (30)$$

from which all the above results, transposed to response functions, can be derived. This is an important remark, since response functions, such as frequency dependent dielectric response or elastic moduli, are routinely measured in glassy materials. Their temperature or density dependence is therefore a direct probe of the dynamic correlation in these materials [37].

#### 3. Higher derivatives

One can of course study higher derivatives of the correlation functions with respect to temperature, which lead to higher order multi-point correlations between dynamics and energy or density fluctuations. For example, the second derivative gives a connected four-point correlation function:

$$\frac{\partial^2 C_o(\mathbf{0},t;T)}{\partial \beta^2} = \int d\mathbf{x}\, d\mathbf{y}\, \langle o(\mathbf{x},t) o(\mathbf{x},0) \delta e(\mathbf{y},0) \delta e(\mathbf{0},0)\rangle_c. \tag{31}$$

The right hand side now defines a squared correlation volume, where the left hand side, computed for $t=\tau_\alpha$, contains terms proportional to $d^2 \ln \tau_\alpha / d \ln T^2$ and to $(d \ln \tau_\alpha / d \ln T)^2$. In most cases where $\ln \tau_\alpha$ diverges as an inverse power of temperature, or in a Vogel-Fulcher-like manner, one finds that the latter term dominates over the former. This means that this squared correlation volume in fact behaves like $\chi_T^2$. The same argument also holds for higher derivatives.

### E. Fluctuations and ensembles

#### 1. Constrained vs. unconstrained fluctuations

The above upper bounds in Eq. (24) can in fact be given a much more precise meaning by realizing that fluctuations of thermodynamic quantities are Gaussian in the large volume limit [58], except at a critical point. This allows one to show the following general result. Consider an observable $O$ that depends on $M$ Gaussian random variables $z_1, z_2, ..., z_M$. We want to compare the ensemble where all the $z_i$'s are free to fluctuate with the ensemble where one constrains a subset of the $z_i$, say $z_m, ..., z_M$ to take fixed values, with no fluctuations. In the limit of small fluctuations, the variances of $O$ in the two ensembles are related through:

$$\Sigma_O^2 = \langle O^2 | z_m, ..., z_M \rangle_c + \sum_{\alpha,\beta=m}^{M} \frac{\partial \langle O | z_m, ..., z_M\rangle}{\partial z_\alpha} \frac{\partial \langle O | z_m, ..., z_M\rangle}{\partial z_\beta} \langle z_\alpha z_\beta \rangle_c, \tag{32}$$

where the average in the ensemble where $z_m, ..., z_M$ are fixed is denoted by $\langle \cdot | z_m, ..., z_M \rangle$. The subscript $c$ means that we consider connected averages and we use Greek indices for the $(M-m+1)$ constrained variables.

Because this result is important throughout this paper, we sketch here its proof, using ideas and a notation which should make clear the analogy with a similar result derived in Sec. III using a field theoretical representation for the dynamics of supercooled liquids. Without loss of generality, we can choose the mean of all $z_i$'s to be zero. The unconstrained joint distribution of the $z_i$'s can be written as:

$$P(\{z_i\}) = \frac{\sqrt{\det D}}{(2\pi)^{M/2}} \exp\left( -\frac{1}{2} \sum_{ij} z_i D_{ij} z_j \right), \tag{33}$$

where $D$ is a certain $M \times M$ symmetric positive definite matrix. The unconstrained covariance between $z_i$ and $z_j$ is well-known to be given by:

$$\langle z_i z_j \rangle = (D^{-1})_{ij}. \tag{34}$$

Let us now write $D$ as blocks corresponding to the $(m-1)$ fluctuating variables and the $(M-m+1)$ fixed variables:

$$D = \begin{bmatrix} A & B \\ B^\dagger & C \end{bmatrix}, \tag{35}$$

where $A$ is $(m-1)\times(m-1)$, $B$ is $(m-1)\times(M-m+1)$ and $C$ is $(M-m+1)\times(M-m+1)$. When the variables $z_m, ..., z_M$ are fixed, the unconstrained variables acquire non-zero average values which are easily found to be given by:

$$\overline{z_i} = \sum_{\alpha=m}^{M} (A^{-1}B)_{i\alpha} z_\alpha. \tag{36}$$

To establish the relation between constrained and unconstrained covariances, we note the following block matrix inversion rule $D^{-1} =:$

$$\begin{bmatrix} \{A - BC^{-1}B^\dagger\}^{-1} & -\{A-BC^{-1}B^\dagger\}^{-1}BC^{-1} \\ -C^{-1}B^\dagger\{A-BC^{-1}B^\dagger\}^{-1} & \{C - B^\dagger A^{-1} B\}^{-1} \end{bmatrix}, \tag{37}$$

together with the matrix identity:

$$\{A - BC^{-1}B^\dagger\}^{-1} = A^{-1} + (A^{-1}B)\{C - B^\dagger A^{-1} B\}^{-1}(A^{-1}B)^\dagger. \tag{38}$$

The constrained covariance $\langle z_i z_j | z_m, ..., z_M \rangle_c$ is clearly given by $(A^{-1})_{ij}$. Using the above identities, we directly obtain:

$$\langle z_i z_j \rangle \equiv \langle z_i z_j | z_m, ..., z_M \rangle_c + \sum_{\alpha,\beta} \frac{\partial \overline{z_i}}{\partial z_\alpha} \frac{\partial \overline{z_j}}{\partial z_\beta} \langle z_\alpha z_\beta \rangle. \tag{39}$$

Now, the final result Eq. (32) above can be established simply by considering, to lowest order in the fluctuations, the observable $O$ as an $M+1$th Gaussian variable correlated with all the $z_i$'s and apply the above equality to $i=j=M+1$.

### 2. From $NPH$ to $NPT$

Let us apply the general result Eq. (32) to the case of interest here, first to the case $M = 1$, with $z_1 = H$ and number of particles fixed. The two ensembles correspond to $NPH$ and $NPT$, respectively. The above formula can be used with the correlation $C_o$ as an observable provided the dynamics is conservative, as argued above. Therefore:

$$\chi_4^{NPT}(\mathbf{r},t) = \chi_4^{NPH}(\mathbf{r},t) + \frac{1}{c_P}\left(\frac{\partial C_o(\mathbf{r},t;T)}{\partial \ln T}\right)_P^2, \quad (40)$$

where we have replaced in the second term in the right hand side $\partial/\partial H$ by $(1/Nc_Pk_B)\partial/\partial T$; $\chi_4^{NPH}(\mathbf{r},t)$ is the variance of the correlation function in the $NPH$ ensemble where enthalpy does not fluctuate, a manifestly non-negative quantity. Therefore, the above equation recovers the lower bound Eq. (24), with a physically explicit expression for the missing piece. The relative contribution of the two terms determining $\chi_4^{NPT}$ will be discussed in concrete cases in Secs. III and V.

### 3. Local vs. global fluctuations

The above discussion may appear puzzling for the following reason: we have seen that the susceptibility $\chi_4(t)$ is the space integral of a four-point correlation function $S_4(\mathbf{y},t)$ which, although developing some spatial correlations on approaching the glass transition, remains relatively short-range in the supercooled liquid phase and should *not* depend on far away boundary conditions that ultimately decide whether energy is conserved or not. Since $S_4(\mathbf{y},t)$ does not depend, in the thermodynamic limit, on the ensemble, how can its integral over space, $\chi_4(t)$, be affected by the choice of ensemble? The answer is that while the finite volume corrections to $S_4(\mathbf{y},t)$ for a given $\mathbf{y}$ tend to zero when $V \to \infty$, the integral over space of these corrections remain finite in that limit [58], and explain the difference between $\chi_4^{NPT}$ and $\chi_4^{NPH}$. We understand that the physical correlation volume is given by $\chi_4^{NPT}$; the long-range nature of the fixed energy constraint leads to an underestimate of $\chi_4$ in the $NPH$ ensemble, which is irrelevant to describe local correlations. This is particularly important in numerical simulations [58]: the study of $S_4(\mathbf{q},t)$ (the Fourier transform of $S_4(\mathbf{y},t)$) in the microcanonical ensemble will lead to a singular behavior associated to the fact that $\lim_{q\to 0} S_4(\mathbf{q},t) \neq S_4(\mathbf{q}=0,t)$, whereas the two coincide only in the ensemble where all conserved quantities are free to fluctuate ($NPH$ for monoatomic liquids). The former quantity is the physical quantity independent of the ensemble and will be denoted $\lim_{q\to 0} S_4(\mathbf{q},t) = \chi_4^*$ in the following, whereas the latter depends on the macroscopic constraint. We summarize this important discussion in Sec. IV.

### 4. Various sources of fluctuations

Equation (32) makes precise the intuition that dynamic fluctuations are partly induced by the fluctuations of quantities that physically affect the dynamic behavior [1, 59]. Among these quantities, some are conserved thermodynamic quantities, such as the energy or density, and the dependence of the dynamics on those quantities are simply measured by the derivatives of the correlation function. The contribution of the local fluctuations of these quantities can therefore be estimated and lead to a lower bound to the total dynamic fluctuations. In a supercooled liquid one expects on general grounds that energy and density should play major roles in the dynamics. From the thermodynamic theory of fluctuations [60], we know that in fact temperature (seen formally as a function of energy and density) and density are independent random variables, with variance $\langle \delta T^2 \rangle = T^2/(Nc_V)$ and $\langle \delta v^2 \rangle = k_BT\kappa_T/(N\rho_0)$. Therefore Eq. (32) gives for the "true" dynamic susceptibility:

$$\chi_4^* = \frac{1}{c_V}\left(\frac{\partial C_o}{\partial \ln T}\right)_V^2 + \rho_0 k_B T \kappa_T \left(\frac{\partial C_o}{\partial \ln \rho}\right)_T^2 + \chi_4^{NVE}, \quad (41)$$

The question of whether other, "hidden" variables also contribute to the dynamic fluctuations is tantamount to comparing $\chi_4^{NVE}$ with $\chi_4^*$. This question is very difficult to resolve theoretically in general. The rest of this paper and the companion paper [38] are devoted to theoretical arguments and numerical simulations which attempt to clarify this issue. Our numerical results suggest that $\chi_4^{NVE} \ll \chi_4^*$, at least close to the glass transition, but that both $\chi_4^{NVE}$ and $\chi_4^*$ are in fact governed by the very same physical mechanism and define the same dynamical correlation length.

Whether energy or density fluctuations is the dominant factor can be assessed by comparing the two explicit terms appearing in the right hand side of Eq. (41). Assuming time-temperature superposition, the ratio $r$ of the two terms for $t = \tau_\alpha$ reads:

$$r = \rho_0 c_V k_B T \kappa_T \left(\frac{\frac{d\ln\tau_\alpha}{d\ln\rho}|_T}{\frac{d\ln\tau_\alpha}{d\ln T}|_\rho}\right)^2. \quad (42)$$

Following Ref. [61], and noting that $\rho_0 c_V k_B T \kappa_T < 1$ in usual liquids, we conclude that for most glass-formers, $r$ is significantly less than one, which means that density effects are weaker than temperature effects and consequently contribute little to dynamic fluctuations. The situation is of course completely the opposite in hard-sphere colloidal glasses, where $d\ln\tau_\alpha/d\ln T|_\rho \to 0$ and $r \gg 1$.

## F. Summary

After motivating the use of multi-point correlation functions to detect non-trivial dynamic correlations in

amorphous materials, we discussed the idea that induced fluctuations are more easily accessible experimentally than spontaneous ones, and can be related to one another by fluctuation-dissipation theorems. Elaborating on this idea, we have shown that the derivative of the correlation function with respect to temperature or density directly gives access to the volume integral of the correlation between local energy (or density fluctuations) and dynamics. This relation can be used to show on very general grounds that a sufficiently abrupt slowing down of the dynamics must be accompanied by the growth of a correlation volume. The detailed relation between these susceptibilities and a correlation lengthscale however depends on the amplitude and spatial structure of the multi-point correlation functions.

We have then shown that the dynamic four-point susceptibility at $q = 0$, which corresponds to the fluctuation of global intensive dynamical correlators, depends in general on the chosen statistical ensemble. In the case where conserved variables are allowed to fluctuate, we showed that the dynamic four-point susceptibility is bounded from below by terms that capture the contribution of energy and density fluctuations to dynamic heterogeneities. Our central results, suggesting a way to estimate a dynamic correlation volume from experiments, are given in Eqs. (24, 41). Whereas we expect that for most supercooled liquids, the contribution of temperature is the dominant effect, the quality of our bounds as quantitative estimators of $\chi_4$, and their physical relevance is, at this stage of the discussion, an open question which we carefully address below, in particular in Sec. IV, and in the companion paper [38]. The following section is devoted to a quantitative study of this question within a field-theory formalism. A surprising outcome of this analysis is that the dynamic four-point susceptibility at $q = 0$ correlations not only depend on the chosen statistical ensemble, as shown above, but also on the choice of microscopic dynamics whether Newtonian or stochastic. Of course the dynamic four-point susceptibility at non-zero $q$ depends only on the choice of microscopic dynamics.

## III. CORRELATION OF DYNAMICAL FLUCTUATIONS: A FIELD-THEORETICAL PERSPECTIVE

In the following we develop in detail an approach to dynamical fluctuations in supercooled liquids based on general field-theory techniques, and discuss how a non-trivial lengthscale can be generated by interactions and manifests itself in quantities like $\chi_4$ or $\chi_T$. We identify precisely the 'susceptibility' (called $A^{-1}$ below) responsible for all interesting dynamic correlations. We discuss the origin of the ensemble dependence of dynamic fluctuations described above from a diagrammatic point of view. This is important since any self-consistent resummation or approximation scheme must be compatible with the bounds derived above. This formalism furthermore predicts that, contrary to the behavior of correlators measuring the average dynamics, the details of dynamic fluctuations depend on the dynamics in a remarkable way. However, since in all cases, the object responsible for the increase of these dynamic correlations is the very same susceptibility $A^{-1}$, the physics revealed by the correlations is independent both of the ensemble and of the dynamics, and genuinely reflects the collective nature of glassy dynamics.

In the companion paper [38] we will point out how simplifications can occur if a true dynamical critical point exists, as within mode-coupling theory, a particular self-consistent resummation scheme. In the following we aim instead at keeping the discussion more general than the confines of mode-coupling theory or any other particular theoretical approach. This is important since mode-coupling theory is not expected to apply close to the glass transition temperature, whereas the present physical conclusions do.

### A. The dynamic field-theory

#### 1. A reminder of the usual static case

The dynamic field-theory strategy is analogous to the one used for ordinary static critical phenomena which we now recall, focusing on the ferromagnetic Ising transition as a pedagogical example [62]. The starting point is the Legendre functional transform $\Gamma(m(\mathbf{x}))$ of the free energy $\beta F(h(\mathbf{x}))$, itself defined as a functional of the magnetic field $h(\mathbf{x})$:

$$\Gamma(m(\mathbf{x})) = \beta F(h(\mathbf{x})) - \int d\mathbf{x}' h(\mathbf{x}') m(\mathbf{x}'), \qquad (43)$$

where $h(\mathbf{x})$ on the right hand side is the field that leads to the magnetization profile $m(\mathbf{x})$. The magnetization is determined via the equation:

$$m(\mathbf{x}) = \frac{\delta \beta F}{\delta h(\mathbf{x})}. \qquad (44)$$

Two important properties of the functional $\Gamma(m(\mathbf{x}))$ that can be directly derived using the previous relation are:

$$\begin{aligned} \frac{\delta \Gamma}{\delta m(\mathbf{x})} &= -h(\mathbf{x}), \\ \frac{\delta^2 \Gamma}{\delta m(\mathbf{x}) \delta m(\mathbf{x}')} &= \frac{\delta h(\mathbf{x})}{\delta m(\mathbf{x}')} \equiv [\langle s(\mathbf{x}) s(\mathbf{x}') \rangle]^{-1}. \end{aligned} \qquad (45)$$

The last exact identity indicates that the operator obtained by differentiating the functional $\Gamma$ twice is the inverse of the spin-spin correlation function (considered as an operator). Note that these are simple generalizations of usual thermodynamic relations.

In general one cannot compute $\Gamma$ exactly, but one can guess its form using symmetry arguments, and compute

it approximately in a perturbative (diagrammatic) expansion in some parameter. Using the above identities, no further approximation is needed to obtain correlation functions. In its simplest version, $\Gamma$ corresponds to the Ginzburg-Landau free energy functional. The saddle point equation for the magnetization then leads to the mean-field description of the transition, whereas the second derivative term gives the mean-field result for the spin-spin correlation function, valid when the space dimensionality is sufficiently large.

In the following, we will present a theory of dynamic fluctuations within a field-theoretic framework similar to the above static formalism. The main difference is that in the context of glassy dynamics, the relevant order parameter is no longer a one-point function like the magnetization but instead a two-point dynamic function which has to be introduced as an effective degree of freedom in the dynamic free-energy functional.

### 2. *Dynamic free-energy functionals and fluctuations*

Different dynamic field-theories have been used in the literature to analyze the dynamics of dense liquids. The common strategy is to write down exact or phenomenological stochastic equations for the evolution of the slow conserved degrees of freedom. For instance, for Brownian dynamics the only conserved quantity is the local density (energy and momentum are not conserved). The equation for the local density is in that case the so-called Dean-Kawasaki equation [63, 64], which can be derived exactly for Langevin particles (see Refs. [65, 66] for a discussion of different field-theories associated with such dynamics). In general, the field-theory associated to a given stochastic dynamics is obtained through the Martin-Siggia-Rose-deDominicis-Janssen method, where one first introduces response fields enforcing the correct time evolution and then averages over the stochastic noise [62, 65].

We will use a general notation that will allow us to treat all field theories proposed in the literature [65, 66] on the same footing. In all those field theories one has a set of slow conserved fields, $\phi_i$ $(i = 1, ..., m)$, and the corresponding response fields, $\hat{\phi}_i$ arising from the Martin-Siggia-Rose procedure [67]. It will also be useful to put $\phi_i, \hat{\phi}_i$ into a single $2m$ dimensional vector $\Phi_a$, $a = 1, ..., 2m$. The average over the dynamic action of $\Phi_a$ will be denoted $\Psi_a$: $\langle \Phi_a \rangle = \Psi_a$. As in the static case, the starting point of the analysis is a Legendre functional (also called the generator of two-particle irreducible diagrams or Baym-Kadanoff functional) [62, 68, 69]. It is equal to:

$$\Gamma(\Psi_a, G_{a,b}) = -\ln \int \mathcal{D}\Phi_a \, \exp\left( -S(\{\Phi_a\}) - \int dt d\mathbf{x} \sum_{a=1}^{2n} h_a(\mathbf{x},t)[\Phi_a(\mathbf{x},t) - \Psi_a(\mathbf{x},t)] \right. \tag{46}$$

$$\left. -\frac{1}{2} \int dt dt' d\mathbf{x} d\mathbf{x}' \sum_{a,b=1}^{2n} K_{a,b}(\mathbf{x},t;\mathbf{x}',t')[\Phi_a(\mathbf{x},t)\Phi_b(\mathbf{x}',t') - \Psi_a(\mathbf{x},t)\Psi_b(\mathbf{x}',t') - G_{a,b}(\mathbf{x},t;\mathbf{x}',t')] \right), \tag{47}$$

where $S$ is the action of the field theory, $h_a$'s are such that $\langle \Phi_a \rangle = \Psi_a$ and $K_{a,b}$ imposes a certain value for the two-point functions: $\langle \Phi_a \Phi_b \rangle - \Psi_a \Psi_b = G_{a,b}$. The properties of $\Gamma(\Psi_a, G_{a,b})$ are the same as in the static case because formally it is the same mathematical object. The only difference is that the dynamical functional depends on a larger number of variables. The difficulty is to devise an approximate expression for the functional $\Gamma$. Once this is done, one should differentiate the functional once to obtain self-consistent equations for the order parameters $\Psi_a, G_{a,b}$ and twice to obtain (after inversion) and expression for their fluctuations. More precisely, we introduce the following matrix of second derivatives:

$$\partial^2\Gamma = \begin{bmatrix} \frac{\delta\Gamma}{\delta G_{a,b}\delta G_{c,d}} & \frac{\delta\Gamma}{\delta G_{a,b}\delta\Psi_e} \\ \frac{\delta\Gamma}{\delta\Psi_f\delta G_{a,b}} & \frac{\delta\Gamma}{\delta\Psi_e\delta\Psi_f} \end{bmatrix} \equiv \begin{bmatrix} A & B \\ B^\dagger & C \end{bmatrix},$$

where we have introduced three block matrices $A, B, C$, in full correspondence with those introduced above in Sec. II E 1. The inversion of $\partial^2\Gamma$ allows one to obtain the objects of interest in this paper. For example, inversion in the "$GG$-sector" defines the four-point space-time correlation functions:

$$(\partial^2\Gamma)^{-1,G}_{a,b;c,d} = \langle (\Phi_a(\mathbf{x},t)\Phi_b(\mathbf{x}',t') - \Psi_a(\mathbf{x},t)\Psi_b(\mathbf{x}',t')) \times (\Phi_c(\mathbf{y},s)\Phi_d(\mathbf{y}',s') - \Psi_c(\mathbf{y},s)\Psi_d(\mathbf{y}',s'))\rangle_c, \tag{48}$$

where $\langle\cdot\rangle_c$ means that we are focusing on the connected component. Similarly, inversion in the "$G\Psi$-sector" defines the three-point functions, such as the energy-correlation correlator defined in the previous section, whereas inversion in the "$\Psi\Psi$-sector" leads to the exact propagators of the conserved quantity. For example, when $\Psi$ is the energy, one obtains the exact energy propagator (dressed by interactions), which is expected to be diffusive in the hydrodynamic limit.

At this stage, it is important to recall that the dynamical functional $\Gamma$ has a direct diagrammatic expression

as [62, 68]:

$$\Gamma(\Psi, G) = -\frac{1}{2}\mathrm{Tr}\log G + \frac{1}{2}\mathrm{Tr}\, G_0^{-1}[G+\Psi\Psi] - \Phi_{2PI}(\Psi, G), \tag{49}$$

where $\Phi_{2PI}(\Psi, G)$ is the sum of all two particle irreducible Feynman diagrams (that cannot be decomposed in two disjoint pieces by cutting two lines) constructed with the vertices of the theory and using the full propagator $G$ as lines and $\Psi$ as sources [62, 68, 69]. Both the internal indices and spatio-temporal arguments were skipped for simplicity. The first derivatives lead to the self-consistent equations for the order parameter. Since in dynamical field-theories for liquids the slow physical fields are in fact conserved quantities the equations $\delta\Gamma/\delta\Psi_a = 0$ do not fix the values of the physical fields that have to be fixed by the initial conditions. On the other hand, they set to zero the average of the response fields and enforce translational invariance [89].

On the other hand, the derivatives $\delta\Gamma/\delta G = 0$ lead to formally exact self-consistent equations for the two-point correlation functions. These equations can be written as a Schwinger-Dyson matrix equation:

$$G^{-1} = G_0^{-1} - \Sigma(G), \qquad \Sigma(G) = \frac{\delta\Phi_{2PI}}{\delta G},$$

where $\Sigma$ is the self-energy. A given approximation consists in retaining a given set of diagrams in $\Phi_{2PI}$, or alternatively in $\Sigma(G)$. For example, mode-coupling theories generically consist in only retaining the "bubble" diagram for $\Sigma(G)$, see Refs. [42, 65, 70] for detailed discussions, and [38] in the present context.

### B. Three-point correlation: dynamic susceptibility and hydrodynamic contributions

From the above general inversion formulas for block matrices, Eq. (37), one can obtain an expression of the inverse of $\partial^2\Gamma$ in the "$G\Psi$-sector" in a form transparent both from physical and diagrammatic standpoints. The off-diagonal block-element of Eq. (37) gives, in particular, the energy-dynamics correlator (see Eq. (16)) and can be rewritten exactly as:

$$S_T \equiv (\partial^2\Gamma)^{-1,G\Psi} = -A^{-1}B\langle\Psi\Psi\rangle, \tag{50}$$

where we have used that $\langle\Psi\Psi\rangle \equiv (\partial^2\Gamma)^{-1,\Psi\Psi}$. Now, the equation determining the two-point correlators is $\delta\Gamma/\delta G = 0$. Therefore the variation of the value of $G$ due to a small variation of $\Psi$, all other parameters being kept fixed, is given by:

$$\frac{\delta G}{\delta\Psi}\delta\Psi = -\left[\frac{\delta^2\Gamma}{\delta G\delta G}\right]^{-1}\frac{\delta^2\Gamma}{\delta G\delta\Psi}\delta\Psi \equiv -A^{-1}B\,\delta\Psi, \tag{51}$$

showing that the operator $\chi_\Psi = -A^{-1}B$ is the response of two-point correlators to a change in conserved quantities. Gathering these results, three-point functions read [90]:

$$S_T = \chi_\Psi\langle\Psi\Psi\rangle, \tag{52}$$

providing an *exact* decomposition with a simple physical meaning. The correlation between energy at one point in space-time and dynamics elsewhere is *governed* by the sensitivity of the dynamics to energy changes, as encapsulated by $\chi_\Psi$, which contains all genuine collective effects in the dynamics induced by interactions. This correlation is *mediated* by energy transport, $\langle\Psi\Psi\rangle$, with has a trivial hydrodynamic structure.

In order to see this more clearly, let us now explore the diagrammatic content of $\chi_\Psi = A^{-1}B$. The three-leg vertex contribution $B = \frac{\delta^2\Gamma}{\delta G\delta\Psi}$ is generically expected to be non singular. The $A^{-1}$ term, on the other hand, can be rewritten using the general expression of $\Gamma$ as:

$$A^{-1} = \left[\frac{\delta^2\Gamma}{\delta G\delta G}\right]^{-1} = \left[G^{-1}G^{-1} - \frac{\delta\Sigma(G)}{\delta G}\right]^{-1},$$

where the objects in the above expression are four-index matrices. This term can be rearranged as follows:

$$\left[\frac{\delta^2\Gamma}{\delta G\delta G}\right]^{-1}_{a,b;c,d} \equiv \sum_{c',d'} G_{a,c'}G_{b,d'} \times \left(\delta_{c',c}\delta_{d',d} - \sum_{c'',d''}\frac{\delta\Sigma_{c'd'}(G)}{\delta G_{c'',d''}}G_{c'',c}G_{d'',d}\right)^{-1}. \tag{53}$$

One can now formally expand the term in parenthesis as $(1-\partial_G\Sigma\, GG)^{-1} = \sum_n(\partial_G\Sigma\, GG)^n$ to recover the so-called "parquet" diagrams [69] that give a formally exact representation of the four-point function, see Fig. 2. This infinite series can provide a divergent contribution (as is the case within MCT at the critical point [17]), signaling the existence of a growing dynamical correlation length and non-trivial collective effects.

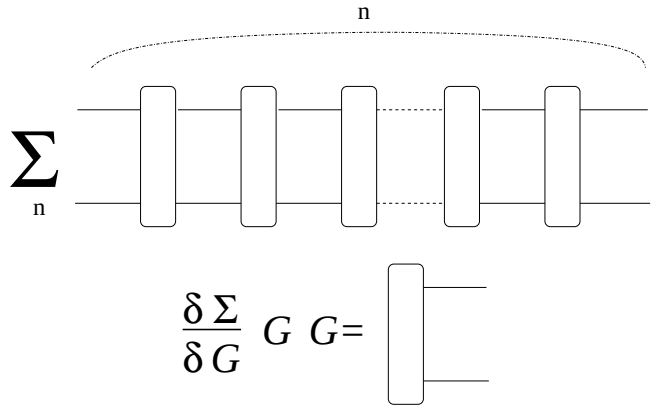


FIG. 2: Diagrammatic representation of the parquet diagrams obtained by expanding Eq. (53): $(1-\partial_G\Sigma\, GG)^{-1} = \sum_n(\partial_G\Sigma\, GG)^n$.

The important conclusion of this section is that the three-point function contains both a long-ranged hydrodynamical contribution $\langle \Psi\Psi \rangle$ related to energy conservation, and an interaction specific contribution – the dynamical susceptibility $\chi_\Psi$. When specializing to the integral over space of the three point function, as in Eq. (16), the contribution of $\langle \Psi\Psi \rangle$ factors out and gives thermodynamic prefactors. This shows that $\partial C/\partial T$ gives in fact a direct access to the dynamical susceptibility $\chi_\Psi$ at $q = 0$. Therefore, the lengthscale extracted from $\partial C/\partial T$ reveals the existence of collective dynamics, and is not related to any thermal diffusion or other hydrodynamical length.

### C. Four-point correlation functions and ensemble dependence

Let us now turn to a similar analysis of the four-point correlations. We start again from the above general inversion formulas for block matrices, Eqs. (37, 38). In the simple case where the $\Psi_a$'s are identically zero by symmetry, as happens for instance in the $p$-spin model for which a gauge symmetry implies that the average value of the spins is always zero, the block matrix $B$ is also zero. Equation (37) then simplifies to:

$$(\partial^2\Gamma)^{-1,G}_{a,b;c,d} = \left[\frac{\delta^2\Gamma}{\delta G_{a,b}\delta G_{c,d}}\right]^{-1} = A^{-1}. \qquad (54)$$

In general this symmetry does not hold, in particular for liquids for which the analysis is more involved. However, it turns out that $A^{-1}$ remains the fundamental object. Using Eq. (38) and the bottom right part of the matrix inversion relation, Eq. (37), the four-point correlation functions can be written in a physically transparent way:

$$(\partial^2\Gamma)^{-1,G}_{a,b;c,d} = \left[\frac{\delta^2\Gamma}{\delta G_{a,b}\delta G_{c,d}}\right]^{-1} + \sum_{e,f}\left(\frac{\delta G_{ab}}{\delta\Psi_e}\langle\Psi_e\Psi_f\rangle_c\left(\frac{\delta G_{cd}}{\delta\Psi_f}\right)^\dagger\right). \qquad (55)$$

This expression parallels Eq. (41) in Sec. II, and the last term corresponds to the dynamic fluctuations induced by the fluctuations of conserved quantities. This formula is however much more general because it applies not only to $\chi_4(t)$ but also to $S_4(q,t)$. Indeed, in Fourier space, the terms contributing to $S_4(q,t)$ read:

$$\langle\delta\rho_{-k_3}(t)\delta\rho_{k_3+q}(0)\delta\rho_{-k_4}(t)\delta\rho_{k_4-q}(0)\rangle. \qquad (56)$$

Therefore the extra contribution from conserved quantities, namely the last term in Eq. (55), reads:

$$\sum_{e,f}\int d\omega \frac{\partial\langle\delta\rho_{-k_3}(t)\delta\rho_{k_3+q}(0)\rangle}{\partial\Psi_e(\omega,q)}\langle\Psi_e(\omega,q)\Psi_f(-\omega,-q)\rangle_c\frac{\partial\langle\delta\rho_{-k_4}(t)\delta\rho_{k_4-q}(0)\rangle}{\partial\Psi_f(-\omega,-q)}. \qquad (57)$$

Now, one should notice that all terms corresponding to indices in the response field sector of $\Psi$ (i.e. $e, f > m$) identically vanish at $q = 0$. The reason is that the response fields always appear in the vertices of the field-theory in the form $\nabla\Psi$. As a consequence, terms like $\delta^2\Gamma/\delta G\delta\Psi_e(\omega,q)$ , for $e > m$, are proportional to $q$ at small $q$.

In the case $q = 0$, the value of conserved fields such as $\Psi_e(\omega,q)$ for $e \leq m$ are by definition constant over time and set by initial conditions: $\langle\Psi_e(\omega,q)\Psi_f(-\omega,-q)\rangle_c = V\delta(\omega)\Sigma_{ef}$ where $\Sigma_{ef}$ are the correlators of thermodynamic fluctuations of all conserved quantities $\Psi$, determined by the probability distribution of initial conditions. As a consequence the term in Eq. (57) at $q = 0$ precisely reduces to the form discussed in the previous section on general grounds for $\chi_4(t) \equiv S_4(q = 0, t)$:

$$\sum_{e,f=1}^{m}\frac{\partial\langle\delta\rho_{-k_3}(t)\delta\rho_{k_3}(0)\rangle}{\partial\Psi_e}\Sigma_{ef}\frac{\partial\langle\delta\rho_{-k_4}(t)\delta\rho_{k_4}(0)\rangle}{\partial\Psi_f}. \qquad (58)$$

For Brownian dynamics, density is the only conserved quantity and thus only one term, $m = 1$, contributes to the sum in Eq. (58). In the case of Newtonian dynamics there are in principle $2 + d$ conserved quantities, density, momentum and energy. However, by symmetry, the contribution of the momentum fluctuations is zero, and only density and energy should be considered. In $p$-spin disordered systems, on the other hand, this extra term is absent, and $m = 0$.

The conclusion is once again that the choice of statistical ensemble matters for determining fluctuations of intensive dynamical correlators which correspond to $q = 0$. For $q \neq 0$, the extra terms Eq. (57) are in general always non-zero and contribute to $S_4(q,t)$. On the other hand, if one focuses on the case where $q = 0$ exactly, the initial distribution is crucial. As an example, in the case of Newtonian dynamics in the $NVE$ ensemble, all the extra contributions vanish since in that ensemble all conserved quantities are strictly fixed and $\Sigma^{NVE}_{ef} \equiv 0$. Thus, we find again within this formalism that the equality $\lim_{q\to 0} S_4(q,t) = S_4(0,t)$ is valid only in the ensemble where all conserved quantities fluctuates. In other ensembles, such as $NVE$, the limit is singular.

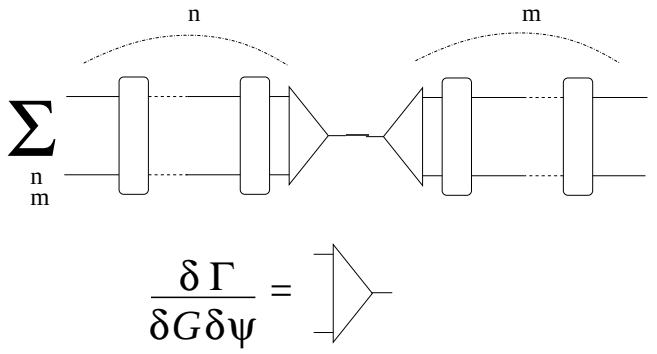


FIG. 3: "Squared-parquets" representation of the contribution of conserved quantity fluctuations to $\chi_4$. They correspond to the second term in Eq. (55).

Let us now explore the diagrammatic content of Eq. (55). The first term was already discussed in the previous section and can be expressed as a sum of parquet diagrams, see Fig. 2. The second term in Eq. (55) also has a direct diagrammatic interpretation, shown in Fig. 3. It consists of two parquets closed by three-leg vertices and joined by a correlation function of conserved variables. The wavevector $q$ in $S_4(q,t)$ is, in the diagrams, the wavevector flowing into the parquets and in the middle "link" corresponding to $\langle \Psi_e \Psi_f \rangle_c$, as it appears explicitly in Eq. (57). A detailed analysis of the structure of the diagrams shows that hydrodynamic scaling between time and length is present only in the middle "link" corresponding to $\langle \Psi_e \Psi_f \rangle_c$.

As discussed in [17], MCT provides a simple approximation in which the self-energy $\Sigma$ is approximated by the "bubble" diagram (see [38]). Within this approximation the parquet diagrams simplify into the ladder diagrams analyzed in [17], which diverge at the mode-coupling critical point. In Ref. [17], however, only the ladder diagrams were analyzed. The contribution to $S_4$ of Eq. (57) corresponding to the "squared ladders" was overlooked. As a consequence the MCT results in Ref. [17] for $\chi_4(t) = S_4(q=0,t)$ only apply close to the critical point in the following cases (see also [38] for further discussion):

- $NVE$ ensemble for Newtonian dynamics;
- $NVT$ ensemble for Brownian dynamics;
- $p$-spin models.

On the other hand, whenever conserved quantities are allowed to fluctuate, or when considering $S_4(q,t)$ at non-zero values of $q$, the contribution of (57) may be important. For example, within the context of MCT where $\chi_\Psi$ diverges as $\epsilon^{-1}$ (where $\epsilon$ is the reduced distance from the critical point), the contribution of (58) in fact becomes dominant and $\chi_4$ for Newtonian dynamics diverges much faster, as $\epsilon^{-2}$. However, see II for a discussion of the application of these MCT results to real systems, where the MCT transition is avoided.

### D. A direct measure of dynamical susceptibility

The analysis of the above sections show that in general $S_4(q,t)$ and $\chi_4(t)$ receive contributions of different physical origin with possibly different temperature dependencies, and whose relative amplitude might even depend on the chosen microscopic dynamics (Brownian or Newtonian). On the other hand, we have seen that all the interesting physics is contained in the fundamental operator $A = [\delta^2\Gamma/\delta G \delta G]$, which governs the growth of dynamic correlations. Therefore it is both of theoretical and practical importance to introduce an observable with a physical content similar to that of $S_4(q,t)$, but unaffected by the presence of global conservation laws and therefore by the choice of statistical ensemble. Such an observable was discussed recently [39]. It corresponds to the response of the intermediate scattering function (the two-point correlator $G$) to a small inhomogeneous external potential $V_{ext}$. Within the previous formalism one writes:

$$\frac{\delta^2\Gamma}{\delta G \delta G}\frac{\delta G}{\delta V_{ext}} + \frac{\delta^2\Gamma}{\delta G \delta V_{ext}} + \frac{\delta^2\Gamma}{\delta G \delta \Psi}\frac{\delta \Psi}{\delta V_{ext}} = 0,$$

and therefore:

$$\frac{\delta G}{\delta V_{ext}} = -A^{-1}\left(\frac{\delta^2\Gamma}{\delta G \delta V_{ext}} + \frac{\delta^2\Gamma}{\delta G \delta \Psi}\frac{\delta \Psi}{\delta V_{ext}}\right).$$

Since the source term on which the operator $A^{-1}$ acts is expected to be only weakly temperature and density dependent, one sees that this quantity gives an almost direct measure of the critical behavior of the dynamic correlations encoded in the operator $A$. When the external potential is homogeneous in space one finds a quantity proportional to $\chi_\Psi$ above [39], while for an inhomogeneous external potential one can probe the full spatial structure of dynamic fluctuations. Indeed, when one differentiates with respect to the Fourier component $V_{ext}(q)$, the wavevector $q$ plays the same role as for $S_4$ [39]. This can be seen at the diagrammatic level because $q$ is the wavevector entering into the ladders in Fig. 3.

## IV. PHYSICAL CONSEQUENCES AND ISSUES

At this stage, it is important to summarize the conclusions drawn from the rather dense theoretical analysis presented above. This will allow us to identify clearly the questions that need to be tested numerically before possibly extrapolating these conclusions to real glass-forming systems.

We established in the previous section that all non-trivial collective dynamical effects are encoded into a certain operator $A^{-1}$, which could in principle be reached by measuring the sensitivity of the local dynamics to an external potential [39]. More easily accessible quantities are derivatives of two-point correlations with respect to temperature, or density. We have shown in detail how

these are indeed proportional to $A^{-1}$ and provide lower bounds on $\chi_4$, and are therefore of direct interest to probe the growth of a dynamic lengthscale in glasses, as claimed in [37]. However, the assumption that growing susceptibilities imply growing lengthscales needs to be discussed more thoroughly.

### A. Growing susceptibilities vs growing lengthscales

The first important remark is that the lower bound on $\chi_4$ obtained in the previous sections is useful only when $\chi_4$ is significantly larger than one because $\chi_4$ is of the order one even in an ideal gas [34]. The second remark is that one has to be sure that the growth of the susceptibility is due to a growing length and not to growing local fluctuations. For simplicity, suppose that the energy-dynamics correlator $S_T(y,\tau_\alpha)$ can be written as $S_T(0) \times y^{2-d-\eta} f(y/\xi)$. Its space integral $\chi_T$ is then given by:

$$\chi_T = S_T(0)\xi^{2-\eta} \int d^d u u^{2-d-\eta} f(u). \qquad (59)$$

This shows the origin of an increase in $\chi_T = \partial C/\partial T$ as $T$ decreases is due to

- either an increase in $\xi$ with a roughly constant $S_T(0)$
- or because $S_T(0)$ increases whereas $\xi$ is trivial,

or, of course, through a combination of both. In order to be confident that the first scenario is the correct one, and that $\chi_T$ can be used to estimate a correlation volume, one needs to be sure that $S_T(0)$ is of order one and basically temperature independent. This requires in principle some extra information, for example on the full spatial dependence of $S_T(y,\tau_\alpha)$. This will be checked in numerical simulations below. We note also that MCT precisely realizes the first scenario above.

From a physical point of view, one expects the enthalpy fluctuations $\delta h$ to contain a fast (kinetic) part and a slow (configurational) part, of similar order of magnitude ($k_B T$). While it is clear that the fast part should have very small correlations with the local correlation on time scale $\tau_\alpha$, there is no reason to think that $\langle o(x,\tau_\alpha) o(x,t=0) \delta h_{slow}(x,t=0)\rangle$ is particularly small. Quite the contrary, we expect that this is of order $k_B T$ in glassy systems. But interestingly, this suggests that the specific heat $c_P$ that should enter the relation between $\chi_T$ and $\xi$ should be the so-called excess specific heat $\Delta c_P$, restricted to slow (glassy) degrees of freedom, as surmised in [37].

### B. Statistical ensemble and dynamics dependence of dynamic fluctuations

A rather bizarre conclusion of the previous section is that global four-point correlators, corresponding to the fluctuations of intensive dynamical correlators, not only depend on the *statistical ensemble* (for $q = 0$) but, remarkably and perhaps unexpectedly, also on the *choice of dynamics*. This is to be contrasted with the case for two-point correlators, which are independent of the chosen ensemble and are known numerically to be independent of the dynamics, at least in the relevant "slow" regime [40, 41, 71]. This shows that four-point correlators, although containing some useful information on dynamical heterogeneities, mixes it with other, less interesting physical effects. Clear-cut statements with four-point quantities can however be made when the dynamic lengthscale grows substantially at some finite temperature or density, as for example within MCT where the operator $A^{-1}$ develops a zero mode that leads to a divergence of the dynamic lengthscale $\xi$. When the dynamic lengthscale becomes very large, these statements may be summarized as follows :

- $\chi_4(\tau_\alpha)$ for $NVT$ Newtonian dynamics diverges more strongly than $\chi_4(\tau_\alpha)$ for $NVT$ stochastic dynamics;
- $\chi_4(\tau_\alpha)$ for $NVE$ Newtonian dynamics diverges like $\chi_4(\tau_\alpha)$ for $NVT$ stochastic dynamics;
- $\chi_4(\tau_\alpha)$ for $NVE$ Newtonian dynamics and $NVT$ stochastic dynamics diverge like $\chi_T(\tau_\alpha)$ (or $\chi_\rho(\tau_\alpha)$).

We will test these statements numerically in the next section, and will indeed establish that $\chi_T$, $\chi_4^{NVE}$ and $\chi_4^B$ increase in exactly the same way with $\tau_\alpha$. The full time dependence of these different correlators will be discussed in the companion paper, Ref. [38].

### C. A unique dynamic correlation length

Let us emphasize again that although $\chi_4(\tau_\alpha)$ for $NVT$ Newtonian dynamics and stochastic dynamics diverge differently, our results strongly suggests these quantities in fact reflect the same underlying physics, which is the growth of a *unique* lengthscale $\xi$ in all of these cases. Only the relation between $\chi_4(\tau_\alpha)$ or $\chi_T(\tau_\alpha)$ and $\xi$ changes: dynamic fluctuations are amplified because of conserved variables. This becomes clear when one considers the (ensemble-independent) function $S_4(q,\tau_\alpha)$ for $q \neq 0$. In all of these cases, $S_4(q,\tau_\alpha)$ can be written as a scaling function $g_4(q\xi)$ with the same $\xi$ but different functional forms. For example, $g_4^N(q\xi)$ for Newtonian dynamics can be written as $g_4^B(q\xi) + c_q [g_4^B(q\xi)]^2$, where $c_q$ is a coefficient and $g_4^B(q\xi) \sim g_T(q\xi)$ the scaling function for Brownian dynamics or governing $S_T(q,\tau_\alpha)$. Note that the relation between $\chi_4(\tau_\alpha)$ for $NVE$ Newtonian dynamics, $\chi_4(\tau_\alpha)$ for $NVT$ Brownian dynamics and $\chi_T(\tau_\alpha)$ may not be accurate far from any critical point, since these quantities are affected by different, non-critical prefactors.

### D. Response vs correlation functions

Four point correlators were originally hoped to be suited to quantify precisely dynamical heterogeneities in glass-formers, as motivated in Sec. II. The conclusion of the previous section and the numerical results of the following ones show that although they contain indeed crucial information, it is mixed up with less interesting physical effects. Nevertheless, a unique dynamic correlation length seems to govern the slowing down independently of the dynamics, global dynamic fluctuations depend on the dynamics and on the ensemble. As discussed formally in the previous section, response functions measuring the response of the dynamics to local perturbations do not present these difficulties. They should be independent of the microscopic dynamics, as it is the case for two-point correlators, and probe directly the dynamic correlations without mixing them up with other effects due to conservation laws.

In the following, we give some numerical evidence for the most important claims made in this paper: the existence of unique lengthscale $\xi$ governing the growth of $\chi_4$ and $\chi_T$ and the ensemble and dynamics dependence of the four-point correlators.

## V. NUMERICAL RESULTS FOR TWO MOLECULAR GLASS-FORMERS

We now present our numerical calculations of the dynamic susceptibility $\chi_T(t)$, its relation to $\chi_4(t)$, and the behavior of spatial correlations $S_T$ and $S_4$ in two well-studied models of molecular glass-formers: a binary Lennard-Jones (LJ) mixture [72], considered as a simple model system for fragile supercooled liquids [9], and the Beest, Kramer, and van Santen (BKS) model, which is a simple description of the strong glass-former silica [73, 74]. A first motivation for these simulations is that all terms contributing to the dynamic fluctuations can be separately evaluated and quantitatively compared. Spatial correlators and dynamic lengthscales can be directly evaluated in the simulations to confirm the link between dynamic susceptibilities and dynamical lengthscales. Therefore, the claim made in Ref. [37] that $\chi_T(t)$ yields direct experimental access to a dynamical lengthscale can be quantitatively established. A second interesting feature is that the influence of the microscopic dynamics and statistical ensemble can be quantified in the simulations by keeping the pair potential unchanged but by switching from the energy conserving Newtonian dynamics to some stochastic dynamics which locally supplies energy to the particles.

### A. Models and technical details

The binary LJ system simulated in this work is a 80:20 mixture of $N_A = 800$ and $N_B = 200$ Lennard-Jones particles of types $A$ and $B$, with interactions

$$\phi^{\rm LJ}_{\alpha\beta}(r) = 4\epsilon_{\alpha\beta}\left[\left(\frac{\sigma_{\alpha\beta}}{r}\right)^{12} - \left(\frac{\sigma_{\alpha\beta}}{r}\right)^{6}\right], \qquad (60)$$

where $\alpha, \beta \in [A, B]$ and $r$ is the distance between the particles of type $\alpha$ and $\beta$. Interaction parameters $\epsilon_{\alpha\beta}$ and $\sigma_{\alpha\beta}$ are chosen to prevent crystallization and can be found in Ref. [72]. The length, energy and time units are the standard Lennard-Jones units $\sigma_{AA}$ (particle diameter), $\epsilon_{AA}$ (interaction energy), and $\tau_0 = \sqrt{m_A\sigma^2_{AA}/(48\epsilon_{AA})}$, where $m_A = m_B$ is the particle mass and the subscript $A$ refers to the majority species. Equilibrium properties of the system have been fully characterized [72]. At the reduced density $\rho_0 = 1.2$, where all our simulations are carried out, the MCT transition has been conjectured to be in the vicinity of $T_c \approx 0.435$ [72]. The slowing down of the dynamics, $T \gtrsim 0.47$, can be correctly described by mode-coupling theory, but this description eventually breaks down when lowering the temperature further, $T \lesssim 0.47$ [72].

To check the generality of our results, we have also investigated the behavior of a second glass-former, characterized by a very different fragility. To this end, we simulate a material with an Arrhenius dependence of its relaxation time, namely silica. Various simulations have shown that a reliable pair potential to simulate silica is the one proposed by BKS [73, 74]. The functional form of the BKS potential is

$$\phi^{\rm BKS}_{\alpha\beta}(r) = \frac{q_\alpha q_\beta e^2}{r} + A_{\alpha\beta}\exp\left(-B_{\alpha\beta}r\right) - \frac{C_{\alpha\beta}}{r^6}, \qquad (61)$$

where $\alpha, \beta \in [{\rm Si}, {\rm O}]$ and $r$ is the distance between the ions of type $\alpha$ and $\beta$. The values of the constants $q_\alpha, q_\beta, A_{\alpha\beta}, B_{\alpha\beta}$, and $C_{\alpha\beta}$ can be found in Ref. [73]. For the sake of computational efficiency the short range part of the potential was truncated and shifted at 5.5 Å. This truncation also has the benefit of improving the agreement between simulation and experiment with regard to the density of the amorphous glass at low temperatures. The system investigated has $N_{\rm Si} = 336$ and $N_{\rm O} = 672$ ions in a cubic box with fixed size $L = 24.23$ Å. The Coulombic part of the potential has been evaluated by means of the Ewald sum using a constant $\alpha L$=10.177.

For both LJ and BKS models we have numerically integrated Newton's equations of motion using the velocity Verlet algorithm [55] using a time-step $h^{\rm LJ} = 0.01\tau_0$ and $h^{\rm BKS} = 1.6$ fs, respectively. Doing so we can measure spontaneous dynamic fluctuations in the microcanonical $NVE$ ensemble. Before these microcanonical production runs, all systems are equilibrated using a stochastic heat bath for a duration significantly longer than the typical relaxation time, $\tau_\alpha$, implying that particles move over several times their own diameter during equilibration. Production runs were at least larger than $30\tau_\alpha$, and statistical convergence for dynamic fluctuations was further improved by simulating 10 independent samples of each system at each temperature. Repeating this strategy for

many temperatures in two molecular systems obviously represents a substantial numerical effort.

To check the influence of the microscopic dynamics, and in particular the role of the energy conservation, we have also performed stochastic simulations of the LJ system using two different techniques. Following Ref. [40], we have simulated Brownian dynamics where Newton's equations are supplemented by a random force and a viscous friction whose amplitudes are related by the fluctuation-dissipation theorem. The numerical algorithm used to integrate these Brownian equations of motion is described in Refs. [40, 55] using the time step of $h_{\rm BD}^{\rm LJ} = 0.016\tau_0$ and a friction coefficient $\zeta = 10m\tau_0$. We use the equilibrium configurations obtained by MD simulations as starting point for our production runs in Brownian simulations. Finally we have implemented a second stochastic dynamics, a standard Monte Carlo dynamics, with the LJ potential [41]. At time $t$, the particle $i$, located at the position $\mathbf{r}_i(t)$, is chosen at random. The energy cost $\Delta E$ to move it to the new position $\mathbf{r}_i(t)+\boldsymbol{\delta}$ is evaluated, $\boldsymbol{\delta}$ being a random vector comprised in a square of lateral size $\delta_{\max} = 0.15$. The Metropolis acceptance rate, $p = \min(1, e^{-\beta\Delta E})$, is then used to decide whether the move is accepted [55]. One Monte Carlo time-step represents $N = N_A + N_B$ attempts to make such a move.

For BKS, we only present results for ND because BD simulations at low enough temperature would be numerically too costly in this system. The reason is that a very large friction coefficient is needed to have a truly damped dynamics [75], making the overall relaxation much too slow to be studied numerically at low temperature. Monte Carlo simulations are similarly slow because of the long-range character of the Coulomb term in the BKS potential. Very recently we have developed a short-range approximation of the BKS potential that allows much faster Monte-Carlo simulations, and we shall mention some preliminary results obtained for dynamic susceptibilities using this method [76].

### B. Physical observables

Following previous work [16, 33, 34], we monitor the dynamical behavior of the molecular liquids through the self-intermediate scattering function,

$$F_s(\mathbf{k},t) = \left\langle \frac{1}{N_\alpha} \sum_{j=1}^{N_\alpha} e^{i\mathbf{k}\cdot[\mathbf{r}_j(t)-\mathbf{r}_j(0)]} \right\rangle, \qquad (62)$$

where the sum in Eq. (62) runs over one of the species of the considered liquid ($A$ or $B$ in the LJ, Si or O for silica). We denote by $f_s(\mathbf{k},t)$ the real part of the instantaneous value of this quantity, so that we have $F_s(\mathbf{k},t) = \langle f_s(\mathbf{k},t)\rangle$.

The four-point susceptibility, $\chi_4(t)$, quantifies the strength of the spontaneous fluctuations around the average dynamics by the variance,

$$\chi_4(t) = N_\alpha \left[\langle f_s^2(\mathbf{k},t)\rangle - F_s^2(\mathbf{k},t)\right]. \qquad (63)$$

In principle, $\chi_4(t)$ in Eq. (63) retains a dependence on the scattering vector $\mathbf{k}$. Since the system is isotropic, we circularly average (62) and (63) over wavevectors of fixed modulus. Note that the value of dynamical correlations depend on $|\mathbf{k}|$ as shown in [32, 36]. A detailed analysis of this dependence has been performed in [53] and will be further discussed in [38]. In the following we will focus only on the value of $|\mathbf{k}|$ for which the dynamical correlations are more pronounced and that measure the correlation of the local dynamics. For the LJ system we will mainly consider results for $|\mathbf{k}| = 7.21$ and for the BKS one $|\mathbf{k}| = 1.7$ Å$^{-1}$. These values respectively represent the typical distance between $A$ particles, and the size of the $SiO_4$ tetrahedra. As discussed above, we expect $\chi_4(t)$ to depend on the chosen statistical ensemble, e.g. $NVE$ or $NVT$, for Newtonian dynamics, and to depend also on which microscopic dynamics is chosen, stochastic or energy conserving.

To evaluate the temperature derivatives involved in

$$\chi_T(t) = \frac{\partial}{\partial T} F_s(\mathbf{k},t), \qquad (64)$$

we perform simulations at nearby temperatures, $T$ and $T+\delta T$, and estimate $\chi_T(t)$ through finite differencing, $\chi_T(t) \approx \delta F_s(k,t)/\delta T$, as illustrated by arrows in Fig. 1 in Sec. II. For this procedure to be effective, temperature differences must be small enough that linear response holds. Taking $\delta T$ too small leads however to poor statistics. The smallest $\delta T$ which might be used can be estimated by comparing the statistical noise of $F_s(k,t)$ to the expected response $\chi_T \times \delta T$. This leads in our case to the typical lower bound $\delta T/T > 0.005$. We have typically used $\delta T/T \approx 0.01$, which is not far from the lower bound. For some selected temperatures, we have explicitly checked that linear response is satisfied by comparing results for $2\delta T$, $\delta T$ and $\delta T/2$.

It might be worth recalling that the value of $\chi_T(t)$ does not depend whether one works in $NVE$ or $NVT$, since ensemble equivalence obviously holds for this local observable [91]. Much less trivial is the numerical finding that $\chi_T(t)$ is also found to be the same for Newtonian, Brownian and Monte Carlo dynamics for times pertaining to the structural relaxation. This directly follows from the non-trivial numerical observation that the average structural relaxation dynamics of the binary LJ system has no dependence upon its microscopic dynamics, apart from an overall time rescaling. On the other hand, the short-time dynamics is different in the three cases. Our findings then confirm for Brownian dynamics, and extend for Monte Carlo dynamics [41], the results of Refs. [40, 71] about the independence of the *average* glassy dynamics upon the microscopic dynamics. We will see below that clear differences emerge at the level of the *dynamic fluctuations*.

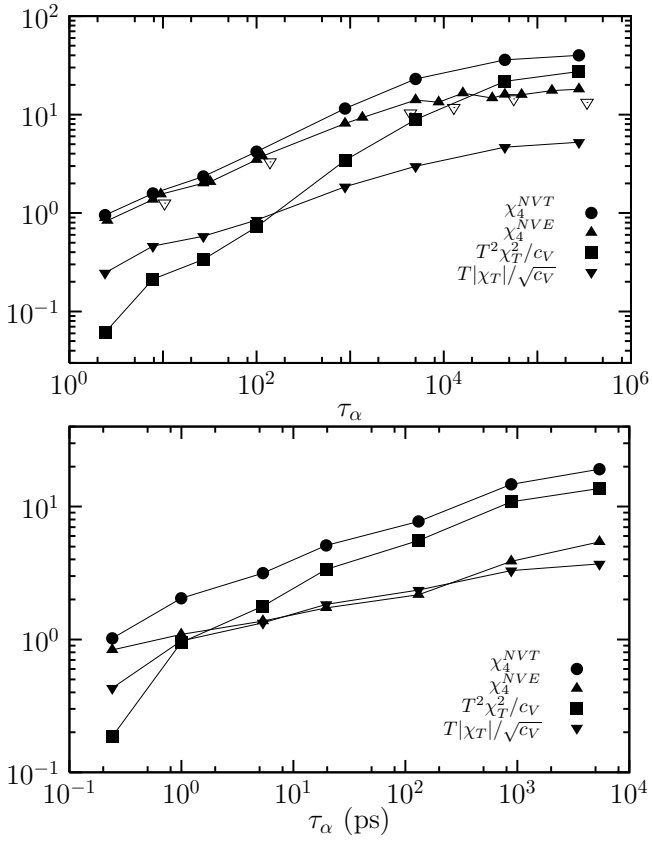


FIG. 4: Peak amplitude of various dynamic susceptibilities in the binary LJ mixture obtained from the $A$ particles dynamics (top) and the BKS model for silica from the Si ions dynamics (bottom). Open triangles in the LJ system represent $\chi_4^{NVE}$ measured in a smaller system with $N = 256$ instead of the $N = 1000$ used everywhere else in the paper. In both cases, $T^2\chi_T^2/c_V$ is smaller than $\chi_4^{NVE}$ at high temperature, but increases faster and becomes eventually the dominant contribution to $\chi_4^{NVT}$ in the relevant low temperature glassy regime. Note that the crossing occurs much earlier for BKS.

### C. Amplitude of the dynamic fluctuations

In this paper, we restrict our analysis of the dynamic susceptibilities to the amplitude of the peaks observed in Fig. 1, meaning that we study dynamic fluctuations on a timescale $t \approx \tau_\alpha$. The time dependence of the fluctuations are studied in the companion paper, Ref. [38].

Furthermore, as discussed in Sec. II E 4, the contribution to $\chi_4^*$ due to density fluctuations in Eq. (41) is significantly less than the one corresponding to energy fluctuations for most molecular liquids. Therefore, we will neglect the role of density fluctuations in the following and focus only on $\chi_4^{NVT}$ since we expect that $\chi_4^{NPT} \simeq \chi_4^{NVT}$. As a more quantitative check, we have used the data in Ref. [83] to estimate that the contribution of density fluctuations to $\chi_4$ is about 10 times smaller than the temperature contribution for the LJ system at $\rho_0 = 1.2$.

#### 1. Ensemble dependence of dynamical correlations

Our results are summarized in Fig. 4, where we present our numerical data for $T|\chi_T|/\sqrt{c_V}$, $\chi_4^{NVE}$, $T^2\chi_T^2/c_V$ and the sum $\chi_4^{NVT} = \chi_4^{NVE} + T^2\chi_T^2/c_V$, all quantities obtained from Newtonian dynamics simulations of both the LJ and BKS models. Recall that we define $c_V$ in units of $k_B$ throughout the paper. When temperature decreases, all peaks shift to larger times and track the $\alpha$-relaxation. Simultaneously, their height increases, revealing increasingly stronger dynamic correlations as the glass transition is approached.

The main observation from the data displayed in Fig. 4, already announced in Ref [37], is that in both LJ and BKS systems the term $T^2\chi_T^2/c_V$ while being small, $\sim O(10^{-1})$, above the onset temperature of slow dynamics, grows much faster than $\chi_4^{NVE}$ when the glassy regime is entered. As a consequence, there exists a temperature below which the temperature derivative contribution to the four-point susceptibility $\chi_4^{NVT}$ dominates over that of $\chi_4^{NVE}$, or is at least comparable. This crossover is located at $T \approx 0.45$ in the LJ system, $T \approx 4500$ K for BKS silica. The conclusion that $T^2\chi_T^2/c_V$ becomes larger than $\chi_4^{NVE}$ at low temperatures holds for both strong and fragile glass-formers, but for different reasons. In the LJ systems $\chi_T$ increases very fast because timescales grow in a super-Arrhenius manner, which makes the temperature derivative larger and larger, while $\chi_4^{NVE}$ saturates at low $T$. In the BKS system, although the temperature derivative is not very large because of the simple Arrhenius growth of relaxation timescales, $\chi_4^{NVE}$ is even smaller [77], i.e. much smaller than in the fragile LJ system. It is interesting to note that the common value of $\chi_4^{NVE}$ and $T^2\chi_T^2/c_V$ when they cross is substantially larger for the LJ system ($\sim 10$) than for BKS ($\sim 1$). It would be interesting to see, more generally, how $\chi_4^{NVE}$ and fragility are correlated.

It is important to remark that finite size effects could play a role in the present study: when measured in a system which is too small, dynamic fluctuations are underestimated [78]. Therefore it could be that using too small a system we have underestimated $\chi_4^{NVE}$, and therefore observed a fictitious saturation of the inequality (24). To investigate this possibility, we have included in Fig. 4 data for $\chi_4^{NVE}$ obtained in a system comprising about 4 times less particles, $N = 256$, with essentially similar results. We have checked that also the average dynamics is unchanged when $N = 256$, so that $\chi_T$ is not affected by finite size effects either for the range of parameters chosen. We are therefore confident that the main conclusion drawn from Fig. 4 is not an artifact due to finite size effects.

We can therefore safely conclude that $T^2\chi_T^2/c_V$ is an excellent approximation to $\chi_4^{NVT}$ for relaxation times larger than $\tau_\alpha \approx 10^4$ in the LJ system, $\tau_\alpha \approx 10$ ps in BKS silica. Our results indicate that this becomes an even better approximation as temperature is lowered, at least in the numerically accessible regime. As reported in

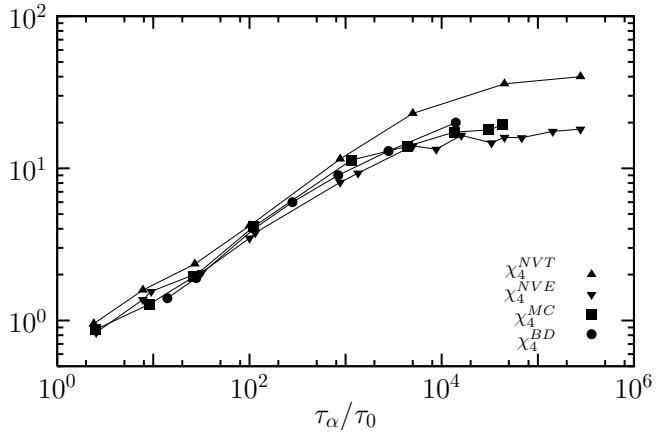


FIG. 5: Amplitude of four-point susceptibilities $\chi_4(\tau_\alpha)$ obtained from the $A$ particles dynamics in the LJ system for Newtonian canonical ($\chi_4^{NVT}$), microcanonical ($\chi_4^{NVE}$) dynamics and stochastic Monte Carlo ($\chi_4^{MC}$) and Brownian ($\chi_4^{BD}$) dynamics. Stochastic dynamics measurements follow the results obtained from microcanonical Newtonian dynamics, while the amplitudes obtained in the canonical ensemble for Newtonian dynamics are much larger, as predicted in Sec. III.

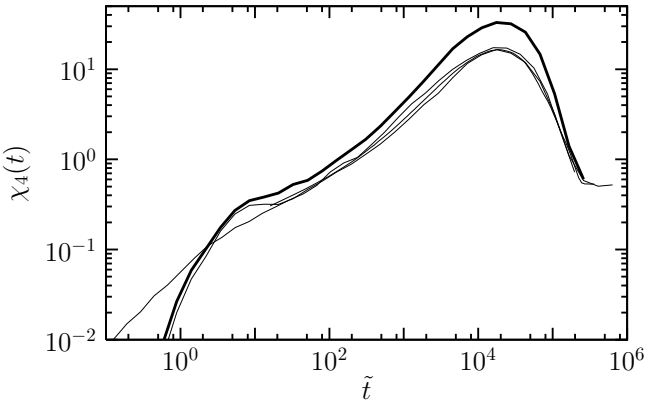


FIG. 6: Four-point susceptibilities at $\chi_4(t)$ at $T = 0.45$ obtained from the $A$ particles dynamics in the LJ system for Newtonian canonical (shown as a thicker line), microcanonical dynamics and stochastic Monte Carlo and Brownian dynamics as a function of a rescaled time chosen so that all $\chi_4$'s overlap near the alpha relation. We chose $\tilde{t} = t$ for $NVE$ Newtonian dynamics, $\tilde{t} = t/24$ for Brownian dynamics, $\tilde{t} = t/100$ for Monte Carlo dynamics. The Newtonian $\chi_4^{NVT}(t)$ is larger than the others, which are all nearly identical in both beta and alpha regimes.

Ref. [37], this suggests a direct experimental determination of $\chi_4$ close to the glass transition temperature, $T_g$. Our data indicate however, that care must be taken when analyzing the first few decades of the dynamical slowing down where all terms contribute differently to $\chi_4^{NVT}$, and have different temperature dependences [37, 53, 79]. We now show that despite their different temperature behavior, $\chi_4^{NVT}$, $\chi_4^{NVE}$ and $\chi_T$ contain the same physics, as predicted theoretically in previous sections.

### 2. *Dynamics dependence of dynamical correlations*

We conclude this section with a discussion of the data for dynamic fluctuations obtained through our stochastic simulations. The temperature evolution of the dynamic susceptibilities $\chi_4(\tau_\alpha)$ obtained with Monte Carlo and Brownian dynamics are shown in Fig. 5 where it is compared to the data obtained in both canonical and microcanonical ensembles with Newtonian dynamics. Our data unambiguously show that dynamic fluctuations with stochastic dynamics are different from the ones obtained with Newtonian dynamics in the $NVT$ ensemble. They are however very similar to the microcanonical ones. This result is not immediately intuitive because one could have imagined that stochastic simulations are a good approximation to the dynamics of liquids in the canonical ensemble. However, we have shown in Sec. III that this naive expectation is in fact incorrect. The absence of the energy conservation in the stochastic dynamics (MD or BD) removes the contribution of the "squared parquets", which corresponds to the enhancement of dynamic fluctuations due to energy fluctuations, and leads to $\chi_4^{NVE} \sim \chi_4^{BD} \sim \chi_4^{MC}$. This is in excellent agreement with our numerical data.

Another confirmation of our theoretical expectations is presented in Fig. 6 in which we show the time dependence of $\chi_4$ for $NVE$ Newtonian dynamics, $NVT$ Brownian, Monte-Carlo and Newtonian dynamics. The first three curves are essentially identical apart at microscopic times, whereas the last one is clearly larger. This dependence on the microscopic dynamics is a general result obtained from the previous diagrammatic discussion.

A further crucial prediction of our diagrammatic analysis is that $\chi_T$ and $\chi_4^{NVE}$ should have a similar critical scaling in temperature and time. This is again a general result if the three-leg vertex does not introduce any additional singular behavior. In fact, as discussed in the previous sections, $\chi_T$ consists of a parquet diagram closed by a three-leg vertex whereas $\chi_4^{NVE}$ is given by single parquet diagrams. In Fig. 4 we confirm numerically that the peaks of $\chi_T$ and $\chi_4^{NVE}$ scale in the same way with the temperature, both in the LJ and BKS systems. This similarity should in fact extend to the whole time dependence but the results are somewhat less satisfactory, as discussed in the companion paper [38].

For BKS we do not have numerical results for Brownian Dynamics for reasons mentioned above. However, our preliminary results from Monte Carlo simulations of a slightly modified version of the BKS potential [76] agree with the conclusions drawn from the LJ data, that is, $\chi_4^{MC}$ seems to follow more closely $\chi_4^{NVE}$, as in Fig. 5, with similar time dependences for the dynamic susceptibilities, as in Fig. 6.

### D. Spatial correlations

We now discuss the spatial correlations associated with the global fluctuations measured through $\chi_T(t)$ and $\chi_4(t)$. To this end, we define the local fluctuations of the dynamics through the spatial fluctuations of the instantaneous value of the self intermediate scattering function,

$$\delta f_k(\mathbf{x},t) = \sum_i \delta(\mathbf{x}-\mathbf{r}_i(0)) \left[\cos[\mathbf{k}\cdot(\mathbf{r}_i(t)-\mathbf{r}_i(0))] - F_s(\mathbf{k},t)\right]. \quad (65)$$

In the following, we will drop the $\mathbf{k}$ dependence of the dynamic structure factors to simplify notations. Local fluctuations of the energy at time $t$ are defined as usual,

$$\delta e(\mathbf{x},t) = \sum_i \delta(\mathbf{x}-\mathbf{r}_i(t)) \left[e_i(t) - e\right], \quad (66)$$

where $e_i(t) = mv_i^2(t)/2 + \sum_j V(r_{ij}(t))$ is the instantaneous value of the energy of particle $i$, and $e \equiv \langle N^{-1}\sum_i e_i\rangle$ is the average energy per particle.

Spontaneous fluctuations of the dynamics can be detected through the "four-point" dynamic structure factor,

$$S_4(\mathbf{q},t) = \frac{1}{N}\langle \delta f(\mathbf{q},t)\delta f(-\mathbf{q},t)\rangle, \quad (67)$$

while correlation between dynamics and energy are quantified by the three-point function,

$$S_T(\mathbf{q},t) = \frac{1}{N}\langle \delta f(\mathbf{q},t)\delta e(-\mathbf{q},t=0)\rangle. \quad (68)$$

In Eqs. (67, 68), $\delta f(\mathbf{q},t)$ and $\delta e(\mathbf{q},t)$ denote the Fourier transforms with respect to $\mathbf{x}$ of $\delta f(\mathbf{x},t)$ and $\delta e(\mathbf{x},t)$, respectively. We will show data for fixed $|\mathbf{k}|$, as for the dynamic susceptibilities above. In our numerical simulations we have also performed a circular averaging over wavevectors of fixed moduli $|\mathbf{q}|$, although the relative orientations of $\mathbf{q}$ and $\mathbf{k}$ plays a role [18, 80].

It should be remarked that the spatial correlations quantified through Eqs. (67, 68) can be measured in any statistical ensemble, because they are local quantities not sensitive to far away boundary conditions. Therefore, their $q \to 0$ limits is related to the dynamic susceptibilities measured in the ensemble where all conserved quantities fluctuate.

We present our numerical results for the temperature dependence of four-point and three-point structure factors in Fig. 7. Similar four-point dynamic structure factor have been discussed before [8, 15, 16, 20, 31, 32, 33, 34]. They present at low $q$ a peak whose height increases while the peak position shifts to lower $q$ when $T$ decreases. This peak is unrelated to static density fluctuations which are small and featureless in this regime [72]. This growing peak is direct evidence of a growing dynamic lengthscale, $\xi_4(T)$, associated to dynamic heterogeneity as temperature is decreased. The dynamic lengthscale $\xi_4$ should then be extracted from these data

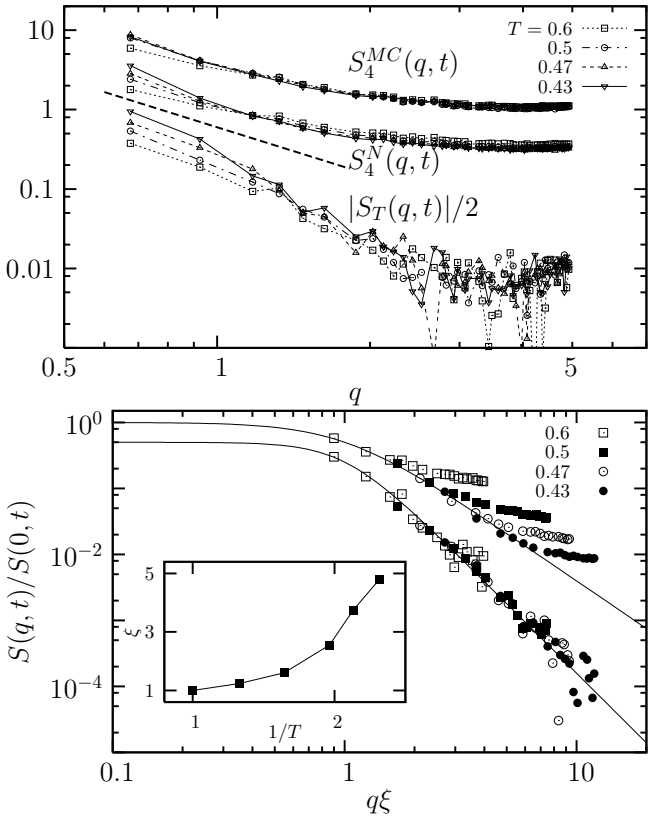


FIG. 7: Top: Four-point dynamic structure factors from Eqs. (67) for Monte Carlo (MC) and Newtonian (N) dynamics, and three-point structure factor, Eq. (68), for Newtonian dynamics. For comparison, we show the power law $1/q^2$ as a dashed line. Note that $S_T$ is a negative quantity, so we present its absolute value. $S_T$ and $S_4^{MC}$ have been vertically shifted for graphical convenience. Bottom: Rescaled dynamic structure factor for Newtonian dynamics using Eq. (69) with $\alpha = 2.4$ for $S_4$ and $\alpha = 3.5$ for $S_T$. The same dynamic lengthscale $\xi_4 = \xi_T \equiv \xi$ is used in both cases, and the temperature evolution of $\xi$ is shown in the inset.

by fitting the $q$-dependence of $S_4(q,t)$ to a specific form. An Ornstein-Zernike form has often been used [32, 33], and we have presented its $1/q^2$ large $q$ behavior in Fig. 7. Since our primary aim is to measure dynamic susceptibilities on a wide range of temperatures, we have used a relatively small number of particles, $N = 1000$. At density $\rho_0 = 1.2$, the largest distance we can access in spatial correlators is $L/2 \approx 5$, which makes an absolute determination of $\xi_4$ somewhat ambiguous. Similarly the range of wavevectors shown in Fig. 7 is too small to assign a precise value even to the exponent characterizing the large $q$ behavior of $S_4(q,t) \sim 1/q^\alpha$. Our data is compatible with a value $\alpha \approx 2.4$. To extract $\xi_4$ we therefore fix $\alpha = 2.4$ and determine $\xi_4$ by assuming the following scaling behavior [34],

$$S_4(q,t) = \frac{S_4(q=0,t)}{1+(q\xi_4)^\alpha}, \quad (69)$$

using $S_4(0,t)$ and $\xi_4$ as free parameters. The results of

such an analysis are shown in the bottom panel of Fig. 7. This procedure leads to values for $\xi_4$ which are in good agreement with previous determinations using different procedures [33]. In particular we find that a power law relationship $\xi_4 \sim \tau_\alpha^{1/z}$ with $z \approx 4.5$ describes our data well, as reported in Ref. [16] for this system.

Since dynamic structure factors probe local spatial correlations they do not depend on the statistical ensemble chosen for their calculation, at least in the thermodynamic limit. However, as predicted in Sec. III, dynamic correlations are expected to retain a dependence on the microscopic dynamics of the particles, our prediction being that correlations should be stronger for Newtonian dynamics than for stochastic dynamics. This prediction is directly confirmed in Fig. 7 where we show $S_4^{MC}(q,t)$ obtained from our Monte Carlo simulations. Clearly the temperature evolution of $S_4^{MC}$ is slower than that of $S_4^{ND}$, in agreement with the slower temperature evolution of $\chi_4^{MC}$ already observed in Fig. 5.

An important new result contained in Fig. 7 is the presence and development of a similar low-$q$ peak in the three-point structure factor $S_T(q,t)$. Note that, as for $\chi_T(t)$, we find that $S_T(q,t)$ is a negative quantity. This means that a local positive fluctuation of the energy is correlated to a local negative fluctuation of the two-time dynamics, i.e. to a locally faster than average dynamics. Therefore the (negative) peak in $S_T(q,t)$ is a direct microscopic demonstration that dynamic heterogeneity is strongly correlated to the fluctuations of at least one local structural quantity, namely the energy [37]. When temperature decreases, the height of the peak in $|S_T(q,t)|$ increases and it shrinks towards lower $q$. This is again the sign of the presence of a second growing dynamic lengthscale, $\xi_T$, which reflects the extent of the spatial correlations between energy and dynamical fluctuations. Again an absolute determination of $\xi_T$ is very hard due to system size limitations. Since we expect $\xi_T$ and $\xi_4$ to carry equivalent physical content, we have checked that our data are compatible with both lengthscales being equal. In Fig. 7, we rescale the three-point dynamic structure factor using Eq. (69) with $\alpha = 3.5$, and constraining $\xi_T = \xi_4$. The scaling is of similar quality, see the bottom panel in Fig. 7. Clearly, the nontrivial $q$-dependence of $S_T(q,t)$ with a scaling collapse of reasonable quality and a length scale consistent with that extracted from $S_4(q,t)$ is a strong indicator that the integrated susceptibility $\chi_T$ grows as a result of a unique growing length scale characteristic of dynamic heterogeneity. A further numerical confirmation of the fact that the growth of the susceptibilities $\chi_4(t)$ and $\chi_T(t)$ cannot be attributed to an increase in the strength of the correlations rather than their range stems from the direct measurement of $g_4(r,t)$ and $g_T(r,t)$, the Fourier transforms of $S_4(q,t)$ and $S_T(q,t)$. The large distance decay of both functions can be well fitted, within the statistical noise, by an exponential form [18] with a growing dynamic lengthscale but a temperature independent strength. Attributing all of the temperature dependence of the susceptibilities to a growing amplitude leads to poor fits of the spatial correlators. This indicates that a scenario whereby the growth of $\chi_T$ can be ascribed to the growth of a prefactor with no growing length scale characteristic of dynamic heterogeneity can be ruled out, at least for the LJ case. Collectively, these findings indicate that the bound for $\chi_4$, as first discussed in [37], correctly estimates a correlation volume associated with dynamic heterogeneity.

We have carried out a similar analysis for the BKS model of silica [76]. Here, the analysis is far more difficult for several reasons. First, the system is harder to simulate than the LJ system due to the long-ranged nature of the interactions. Second, strong features associated with static structure make a resolution of the low-$q$ behavior in $S_T(q,t)$ somewhat more challenging in this system. Lastly, the overall scale of dynamical fluctuations at the lowest temperatures studied are much smaller than in the LJ system (see Fig. 4). Regardless, we do find results consistent with a scaling scenario for $S_T(q,t)$, and, as we will see in the following paper, the growth of $\chi_T$ tracks that of $\chi_4^{NVE}$. These facts give support to the notion that the scenario for the BKS model of silica is the same as for the LJ system although the direct supporting evidence for this is, at this stage, not quite as strong.

The local correlation between energy fluctuations dynamic heterogeneity is broadly consistent with several theoretical predictions; see the companion paper [38] for further discussion. As mentioned in Sec. III the equality between $\xi_T$ and $\xi_4$ is a natural prediction, in particular close to the MCT transition. This is also very natural from the point of view of kinetically constrained models [44]. Spin facilitated models, in particular, *postulate* such a correlation through the concept of dynamic facilitation: mobile sites carry positive energy fluctuations and through activated diffusion trigger the relaxation of neighboring sites [81]. In this picture a localized energy fluctuation affects the dynamics of a large nearby region so that there is not a one-to-one correspondence between slow and low-energy sites. There is therefore no contradiction between our results and the lack of correlation between "dynamic propensity" and local potential energy recently reported in Ref. [82]. They qualitatively agree, however, with recent numerical results obtained for water where a correlation between "dynamic" and "energetic" propensities is reported [84]. A recent work [85] has also suggested a relation between energy fluctuations and finite size effects leading to a growing length at low temperature.

### E. Summary

In this section we have discussed in detail the results of molecular dynamics simulations of a strong and a fragile glass-forming liquid. Our main contribution is the simultaneous measurement of spontaneous and induced dynamic fluctuations, and the quantitative confirmation in two realistic liquids of the central claim announced

in Ref. [37]: it is possible to obtain a quantitative estimate of the amplitude of dynamic fluctuations in supercooled liquids through the measurement of the quantity $T\chi_T/\sqrt{c_V}$, which (once squared) gives the major contribution to $\chi_4^{NVT}$, and hence to $\chi_4^{NPT}$, in the low temperature regime, and is proportional to $\chi_4^{NVE}$: see Fig. 4.

We have directly measured in the Lennard-Jones system three- and four-point dynamic structure factors that display slightly different wavevector dependences but lead nevertheless to consistent quantitative estimates of a dynamic correlation lengthscale, compatible with that obtained from $\chi_4$ and $\chi_T$. This last result is very important since this is direct confirmation that an experimental estimate of a dynamic lengthscale, as performed in Ref. [37], is meaningful. Finally, we have found that, as predicted theoretically, global four-point dynamic correlations corresponding to spontaneous fluctuations of two-time correlators are strongly dependent on the microscopic dynamics, at variance with usual two-point correlations.

## VI. PERSPECTIVES AND CONCLUSIONS

We conclude this rather long article, to be followed by a companion paper [38], with brief comments only. Four-point correlators were originally introduced to define the lengthscale of dynamical heterogeneities in glass formers. Our results, in that respect, are double-sided. We showed that global four-point functions, corresponding to the fluctuations of intensive dynamical correlators, not only depend on the statistical ensemble but also on the choice of dynamics. The dependence on the statistical ensemble is useful to obtain lower bounds for experimentally relevant situations. However, on a more general ground, these dependences unveil that four-point correlators are more complicated than what was originally thought and their quantitative interpretation is somewhat flummoxed. Instead, we found that dynamical response functions, proxied by the temperature or density derivatives of two-time correlators provide a more clear and direct probe of genuine collective dynamical effects.

We have given strong theoretical and numerical evidence for the most important claim made in this paper: the existence of unique dynamical lengthscale $\xi$ governing the growth of all the relevant dynamical susceptibilities, independently of dynamics (and of course ensemble!). This result can be proved within the MCT of glasses, as we elaborate further in the companion paper [38], but is expected more generally as soon as $\xi$ becomes somewhat large compared to the inter-atomic spacing. Our numerical results show that this is true both in the fragile LJ system and in the strong BKS system: all dynamical susceptibilities ($\chi_T$, $\chi_4^{NVE}$) behave similarly, at least in the weakly supercooled region accessible to numerical simulations.

One rather striking result of our analysis is that even Arrhenius dynamics in Newtonian systems must involve some amount of dynamical correlations. This is confirmed by our numerical simulations on the BKS system, but the result holds more generally. Even a dilute assembly of Arrheniusly relaxing entities, e.g. two-level systems, should develop non-trivial dynamical correlations at sufficiently low temperatures, provided they interact with the *same* Newtonian thermal bath. This is obviously the case for a strong glass-formers where a particle is both a relaxing entity and part of its neighbors' bath.

As for the perspective for the future, we hope that our work will trigger more experimental and numerical investigations of supercooled liquids and jamming systems, extending our results both from a quantitative and a qualitative point of view [45]. In particular, the distinction between dynamical correlations (explored here) and cooperativity, if any, should be clarified. The relation between the two notions might be very different in strong and fragile systems, and the distinction between the MCT and the deeply supercooled regimes might also be relevant. Is $\xi$ as defined in the present paper related to the Adam-Gibbs or the mosaic length scale [10, 86]? In this respect, the full understanding of deceivingly simple Arrhenius systems should be of great help.

### Acknowledgments

We thank L. Cipelletti, S. Franz, F. Ladieu, A. Lefèvre, D. L'Hôte and G. Szamel for discussions. We are also deeply indebted to M. Cates and G. Tarjus for insightful remarks which helped clarifying the manuscript. D.R.R. and K.M. acknowledge support from the NSF (NSF CHE-0134969). G.B. is partially supported by EU contract HPRN-CT-2002-00307 (DYGLAGEMEM). K.M. would like to thank J. D. Eaves for his help on the development of efficient numerical codes.

[1] E. Donth, *The glass transition* (Springer, Berlin, 2001).
[2] P. G. Debenedetti, F. H. Stillinger, Nature **410**, 259 (2001).
[3] K. Binder and W. Kob, *Glassy materials and disordered solids* (World Scientific, Singapore, 2005).
[4] R. Leheny, N. Menon, S. R. Nagel, D. L. Price, K. Suzuya, and P. Thiyagarajan, J. Chem. Phys. **105**, 7783 (1996); A. Tolle, H. Schober, J. Wuttke, and F. Fujara, Phys. Rev. E, **56**, 809 (1997).
[5] M. D. Ediger, Annu. Rev. Phys. Chem. **51**, 99 (2000).
[6] H. Sillescu, J. Non-Cryst. Solids **243**, 81 (1999).
[7] R. Richert, J. Phys.: Condens. Matter **14**, R703 2002 .
[8] S. C. Glotzer, J. Non-Cryst. Solids **274** 342 (2000).
[9] H. C. Andersen, Proc. Natl. Acad. Sci. **102**, 6686 (2005).

[10] X. Y. Xia and P. G. Wolynes, Proc. Natl. Acad. Sci. **97**, 2990 (2000).

[11] P. Viot, G. Tarjus, D. Kivelson, J. Chem. Phys. **112**, 10368 (2000).

[12] J. Jäckle and S. Eisinger, Z. Phys. B: Condens. Matter **84**, 115 (1991).

[13] G. H. Fredrickson and H. C. Andersen, Phys. Rev. Lett. **53**, 1244 (1984); J. Chem. Phys. **83**, 958 (1984).

[14] S. Butler and P. Harrowell, J. Chem. Phys. **95**, 4454 (1991); **95**, 4466 (1991); P. Harrowell, Phys. Rev. E **48**, 4359 (1993); M. Foley and P. Harrowell, J. Chem. Phys. **98**, 5069 (1993).

[15] J. P. Garrahan, D. Chandler, Phys. Rev. Lett. **89**, 035704 (2002).

[16] S. Whitelam, L. Berthier, J. P. Garrahan, Phys. Rev. Lett. **92**, 185705 (2004); Phys. Rev. E **71**, 026128 (2005).

[17] G. Biroli and J.-P. Bouchaud, Europhys. Lett. **67**, 21 (2004).

[18] B. Doliwa and A. Heuer, Phys. Rev. E **61**, 6898 (2000).

[19] M. M. Hurley and P. Harrowell, Phys. Rev. E **52**, 1694 (1995); D. N. Perera and P. Harrowell, J. Chem. Phys. **111**, 5441 (1999).

[20] R. Yamamoto and A. Onuki, Phys. Rev. Lett. **81**, 4915 (1998).

[21] Y. Hiwatari and T. Muranaka, J. Non-Cryst. Solids **235-237**, 19 (1998).

[22] U. Tracht, M. Wilhelm, A. Heuer, H. Feng, K. Schmidt-Rohr, and H. W. Spiess, Phys. Rev. Lett. **81**, 2727 (1998).

[23] E. Weeks, J.C. Crocker, A.C. Levitt, A. Schofield, and D.A. Weitz, Science **287**, 627 (2000).

[24] E. Vidal-Russell, N. E. Israeloff, Nature **408**, 695 (2000).

[25] S. A. Reinsberg, X. H. Qiu, M. Wilhelm, H. W. Spiess, and M. D. Ediger, J. Chem. Phys. **114**, 7299 (2001).

[26] X. H. Qiu and M. D. Ediger, J. Phys. Chem. B **107**, 459 (2003).

[27] E. Hempel, G. Hempel, A. Hensel, C. Schick, and E. Donth, J. Phys. Chem. B **104**, 2460 (2000).

[28] S. Franz, G. Parisi, J. Phys.: Condens. Matter **12**, 6335 (2000).

[29] G. Parisi, J. Phys. Chem. B **103**, 4128 (1999).

[30] S. Franz, C. Donati, G. Parisi, and S. C. Glotzer, Phil. Mag. B, **79**, 1827, (1999); C. Donati, S. Franz, S. C. Glotzer, and G. Parisi, J. Non-Cryst. Solids **307**, 215 (2002).

[31] C. Bennemann, C. Donati, J. Baschnagel, S. C. Glotzer, Nature **399**, 246 (1999).

[32] N. Lačević, F. W. Starr, T. B. Schroder, and S. C. Glotzer, J.Chem.Phys. **119**, 7372 (2003).

[33] L. Berthier, Phys. Rev. E **69**, 020201 (2004).

[34] C. Toninelli, M. Wyart, G. Biroli, L. Berthier, J.-P. Bouchaud, Phys. Rev. E **71**, 041505 (2005).

[35] P. Mayer, H. Bissig, L. Berthier, L. Cipelletti, J. P. Garrahan, P. Sollich, and V. Trappe, Phys. Rev. Lett. **93**, 115701 (2004).

[36] O. Dauchot, G. Marty and G. Biroli, Phys. Rev. Lett. **95**, 265701, (2005).

[37] L. Berthier, G. Biroli, J.-P. Bouchaud, L. Cipelletti, D. El Masri, D. L'Hôte, F. Ladieu, and M. Pierno, Science **310**, 1797 (2005).

[38] L. Berthier, G. Biroli, J.-P. Bouchaud, W. Kob, K. Miyazaki, and D. R. Reichman, companion paper, cond-mat/0609658.

[39] G. Biroli, J.-P. Bouchaud, K. Miyazaki, and D. R. Reichman, Phys. Rev. Lett. **97**, 195701 (2006).

[40] T. Gleim, W. Kob, and K. Binder, Phys. Rev. Lett. **81**, 004404 (1998).

[41] L. Berthier and W. Kob, to be published in J. Phys. Condens. Matter, condmat/0610253.

[42] J.-P. Bouchaud, L. F. Cugliandolo, J. Kurchan and M. Mézard, Physica A **226**, 243 (1996).

[43] W. Götze, J. Phys. Cond. Matt. **11**, A1 (1999). W. Götze and L. Sjögren, Rep. Prog. Phys. **55**, 241 (1992).

[44] F. Ritort and P. Sollich, Adv. Phys. **52**, 219 (2003).

[45] C. Alba-Simionesco, L. Berthier, G. Biroli, J.-P. Bouchaud, C. Dalle-Ferrier, D. L'Hôte, F. Ladieu, G. Tarjus, C. Thibierge, in preparation.

[46] R. M. Ernst, S. R. Nagel, and G. S. Grest, Phys. Rev. B **43**, 8070, (1991).

[47] K. Binder and A. P. Young, Rev. Mod. Phys. **58**, 801 (1986).

[48] S. F. Edwards and P. W. Anderson, J. Phys. F : Metal Phys. **5** 965 (1975).

[49] J.-P. Bouchaud, G. Biroli, Phys. Rev. B **72** 064204 (2005).

[50] This was recently shown rigourously for a large class of glassy dynamics in A. Montanari, G. Semerjian, J. Stat. Phys. **125**, 22 (2006), and suggested in full generality by the bound derived in [37].

[51] J. P. Hansen, I. R. Mc Donald, *Theory of simple liquids* (Elsevier, Amsterdam, 1986).

[52] T. R. Kirkpatrick and D. Thirumalai, Phys. Rev. A **37**, 4439 (1988).

[53] D. Chandler, J. P. Garrahan, R. L. Jack, L. Maibaum and A. C. Pan, Phys. Rev. E **74**, 051501 (2006).

[54] L. Cipelletti and L. Ramos, J. Phys. : Condens. Matter **17**, R253 (2005).

[55] M. Allen and D. Tildesley, *Computer Simulation of Liquids* (Oxford University Press, Oxford, 1987).

[56] B. Doliwa and A. Heuer, Phys. Rev. E **61**, 6898 (2000).

[57] P. N. Pusey, W. van Megen, Nature **320**, 340 (1986).

[58] J. L. Lebowitz, J. K. Percus, L. Verlet, Phys. Rev. **153**, 250 (1967).

[59] M. D. Ediger, J. Non-Cryst. Solids **235-237**, 10 (1998).

[60] L. D. Landau and E. M. Lifshitz, *Statistical Physics, Course of Theoretical Physics, Vol. 5, Pt. 1* (Pergamon, New York, 1980).

[61] G. Tarjus, D. Kivelson, S. Mossa, C. Alba-Simionesco, J. Chem. Phys. **120**, 6135 (2004).

[62] J. Zinn Justin, *Quantum field theory and critical phenomena* (Oxford University Press, Oxford, 2002).

[63] D. S. Dean, J. Phys. A **29**, L613 (1996).

[64] K. Kawasaki, Phyisica A **208**, 35 (1994).

[65] A. Andreanov, G. Biroli, and A. Lefèvre, J. Stat. Mech. P07008 (2006).

[66] S. P. Das, Rev. Mod. Phys. **76**, 785 (2004).

[67] J. Cardy, *Scaling and Renormalization in Statistical Physics* (Cambridge University Press, Cambridge, 1996).

[68] C. De Dominicis and P. Martin, J. Math. Phys. **5**, 14 and 31 (1964).

[69] J.-P. Blaizot, G. Ripka, *Quantum Theory of Finite Systems* (Editions Phenix, Kiev, 1998).

[70] K. Miyazaki and D. R. Reichman, J. Phys. A: Math. Gen. **38**, L343 (2005).

[71] G. Szamel, and E. Flenner, Europhys. Lett. **67**, 779 (2004).

[72] W. Kob and H. C. Andersen, Phys. Rev. Lett. **73**, 1376 (1994); Phys. Rev. E **53**, 4134 (1995); Phys. Rev. E **51**, 4626 (1995).

[73] B. W. H. van Beest, G. J. Kramer, and R. A. van Santen, Phys. Rev. Lett. **64**, 1955 (1990).
[74] S. N. Taraskin and S. R. Elliott, Europhys. Lett. **39**, 37 (1997); M. Benoit, S. Ispas, P. Jund, and R. Jullien, Eur. Phys. J. B **13**, 631 (2000); J. Horbach and W. kob, Phys. Rev. B **60**, 3169 (1999); Phys. Rev. E **64**, 041503 (2001).
[75] J. Horbach and W. Kob, unpublished.
[76] L. Berthier, unpublished.
[77] M. Vogel and S. C. Glotzer, Phys. Rev. Lett. **92**, 255901 (2004); Phys. Rev. E **70**, 061504 (2004).
[78] L. Berthier, Phys. Rev. Lett. **91**, 055701 (2003).
[79] G. Szamel and E. Flenner, Phys. Rev. E **74**, 021507 (2006).
[80] E. Flenner, G. Szamel, cond-mat/0608398.
[81] J. P. Garrahan and D. Chandler, Proc. Natl. Acad. Sci. **100**, 9710 (2003); L. Berthier and J. P. Garrahan, Phys. Rev. E **68**, 041201 (2003).
[82] A. Widmer-Cooper, P. Harrowell, and H. Fynewever, Phys. Rev. Lett. **93**, 135701 (2004); A. Widmer-Cooper and P. Harrowell, Phys. Rev. Lett. **96**, 185701 (2006).
[83] S. Sastry, Phys. Rev. Lett. **85**, 590 (2000).
[84] G. S. Matharoo, M. S. G. Razul, and P. H. Poole, Phys. Rev. E **74**, 050502 (2006).
[85] L.A. Fernandez, V. Martin-Mayor and P. Verrocchio Phys. Rev. E **73**, 020501 (2006).
[86] J.-P. Bouchaud and G. Biroli, J. Chem. Phys. **121**, 7347 (2004).
[87] A similar expression could be obtained when $C_o(\mathbf{r},t)$ is computed using a time average instead of a space average; the resulting variance would now measure the temporal correlation of the temporal correlation.
[88] Note that for the enthalpy we use the notation $H(t=0)=\frac{1}{N}\int d\mathbf{x}h(\mathbf{x},t=0)$. Therefore, $h$ is an enthalpy per unit volume.
[89] Note that since the value of the physical fields is fixed by the initial conditions and not changed by loop corrections, it is often more useful and practical to develop the theory in terms of $\delta\Psi$ so that the average of the fluctuating fields is zero by construction.
[90] The following identity can also be seen as a Novikov formula for Gaussian fluctuations.
[91] Note, however, that in general one has to be careful that the derivative with respect to temperature is performed keeping the same other variables fixed.